Author Manuscript

Author Manuscript

Author Manuscript

Author Manuscript

HHS Public Access

Author manuscript

Cell Rep. Author manuscript; available in PMC 2021 August 05.

Published in final edited form as:

Cell Rep. 2021 July 20; 36(3): 109419. doi:10.1016/j.celrep.2021.109419.

Tau oligomer induced HMGB1 release contributes to cellular senescence and neuropathology linked to Alzheimer's disease and frontotemporal dementia

Sagar Gaikwad[1,2], **Nicha Puangmalai**[1,2], **Alice Bittar**[1,2], **Mauro Montalbano**[1,2], **Stephanie Garcia**[1,2], **Salome McAllen**[1,2], **Nemil Bhatt**[1,2], **Minal Sonawane**[1,2], **Urmi Sengupta**[1,2], **Rakez Kayed**[1,2,3,*]

[1]Mitchell Center for Neurodegenerative Diseases, University of Texas Medical Branch, Galveston, TX 77555, USA

[2]Departments of Neurology, Neuroscience, and Cell Biology, University of Texas Medical Branch, Galveston, TX 77555, USA

[3]Lead contact

SUMMARY

Aging, pathological tau oligomers (TauO), and chronic inflammation in the brain play a central role in tauopathies, including Alzheimer's disease (AD) and frontotemporal dementia (FTD). However, the underlying mechanism of TauO-induced aging-related neuroinflammation remains unclear. Here, we show that TauO-associated astrocytes display a senescence-like phenotype in the brains of patients with AD and FTD. TauO exposure triggers astrocyte senescence through high mobility group box 1 (HMGB1) release and inflammatory senescence-associated secretory phenotype (SASP), which mediates paracrine senescence in adjacent cells. HMGB1 release inhibition using ethyl pyruvate (EP) and glycyrrhizic acid (GA) prevents TauO-induced senescence through inhibition of p38-mitogen-activated protein kinase (MAPK) and nuclear factor κB (NF-κB)—the essential signaling pathways for SASP development. Despite the developed tauopathy in 12-month-old hTau mice, EP+GA treatment significantly decreases TauO and senescent cell loads in the brain, reduces neuroinflammation, and thus ameliorates cognitive functions. Collectively, TauO-induced HMGB1 release promotes cellular senescence and neuropathology, which could represent an important common pathomechanism in tauopathies including AD and FTD.

In brief

This is an open access article under the CC BY-NC-ND license (http://creativecommons.org/licenses/by-nc-nd/4.0/).

*Correspondence: rakayed@utmb.edu.

AUTHOR CONTRIBUTIONS

Conceptualization, S.G. and R.K.; methodology, S.G. and R.K.; investigation, S.G., N.P., N.B., A.B., M.M., S.M., N.B., U.S., S.G., and R.K.; writing – original draft, S.G.; writing – review & editing, all authors; funding acquisition, R.K.; resources, R.K.; supervision, S.G. and R.K.

SUPPLEMENTAL INFORMATION

Supplemental information can be found online at https://doi.org/10.1016/j.celrep.2021.109419.

DECLARATION OF INTERESTS

The authors declare no competing interests.

Author Manuscript Author Manuscript Author Manuscript Author Manuscript

Gaikwad et al. demonstrate that TauO-associated astrocytes exhibit senescence-like phenotype in the brain of patients with AD and FTD. They find that HMGB1 release is a crucial event for TauO-induced cellular senescence, tauopathy progression, and cognitive deficits, indicating that HMGB1 release could represent an important common pathomechanism in tauopathies.

Graphical Abstract

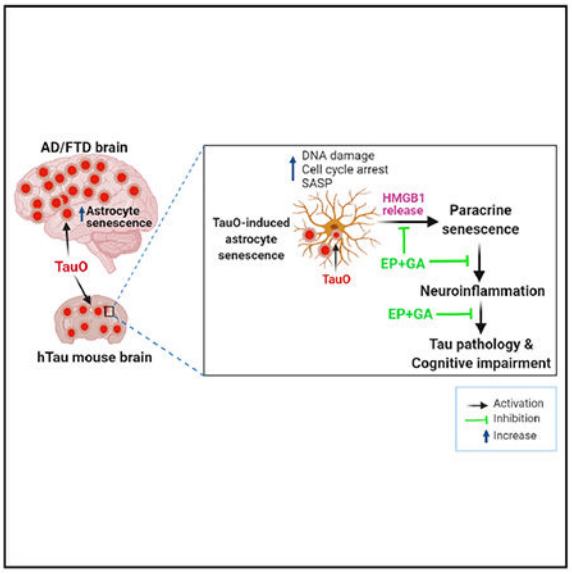

INTRODUCTION

Tauopathies including Alzheimer's disease (AD) and frontotemporal dementia (FTD) are "aging-associated" progressive neurodegenerative disorders, characterized by deposition of tau aggregates in the brain and cognitive deficits for which there are no disease-modifying regimens to date. Chronic neuroinflammation is also an important contributor to the pathogenesis and progression of tauopathies (Guzman-Martinez et al., 2019). Current challenges for the tauopathy treatment include incomplete understanding of the mechanisms involved in aging-related and pathological tau-mediated chronic neuroinflammation, neuronal loss, and cognitive dysfunctions. Various therapeutic strategies have been tested in clinical trials for AD and showed unsatisfactory results (Doody et al., 2013,2014; Golde et al., 2011). These results have shifted research interests on pathological tau aggregates and chronic neuroinflammation—the other hallmarks of the disease (Guzman-Martinez et al., 2019; Lasagna-Reeves et al., 2012). Neurons with neurofibrillary tangles (NFTs) can survive for decades (Morsch et al., 1999), while tau oligomers (TauO) were identified as the most neurotoxic tau species that elicits cognitive impairments (Lasagna-Reeves et al., 2012; Shafiei et al., 2017), suggesting that pathogenic TauO plays a crucial role in the etiology of tauopathies. Pathological tau can be secreted by neurons into extracellular space both *in vitro* and *in vivo* (Pernègre et al., 2019). Extracellular tau can be internalized by neighboring cells, both neurons and glial cells, via endocytic, pinocytic, and phagocytic mechanisms, contributing to the propagation of tau pathology between the anatomically connected brain regions (Puangmalai et al., 2020; Zhao et al., 2021). Previously, we reported elevated levels

Author Manuscript Author Manuscript Author Manuscript Author Manuscript

of TauO in cerebrospinal fluid (CSF) of AD patients compared with age-matched non-demented controls (NDCs; Sengupta et al., 2017), supporting the notion that TauO is extracellularly released in AD. Studies have shown that extracellular TauO secretion is an early event during brain aging and neurodegeneration (Maeda et al., 2006), and increased tau levels in CSF correlate with clinical severity in AD patients (Andreasen et al., 2001; Sengupta et al., 2017). Given that astrocytes express very low or undetectable levels of tau, its presence in the astrocytes during tauopathies can be explained by the internalization of pathological tau from the extracellular space (Forman et al., 2005; Kovacs et al., 2017a; Zhang et al., 2016). Consequently, this astrocytic internalization of tau may contribute to the pathological spread of tau (Hyman, 2014; Rauch et al., 2020). The tau accumulation in astrocytes of the dentate gyrus effectively induces neuronal dysfunction and memory deficits (Richetin et al., 2020). These findings suggest a critical role of extracellular tau and astrocytes in tau pathology. While TauO's impact on neurons has been extensively investigated, the effect of extracellular TauO on astrocytes and aging-associated neuroinflammation remains unclear.

Astrocytes are the highly abundant glial cells found in the brain. They play a critical role in the regulation of neuronal homeostasis, neuroinflammation, and synaptic and cognitive functions (Vasile et al., 2017). In healthy brains, astrocytes are involved in various physiological functions including protection and differentiation of neurons, ion homeostasis, neurotransmitter release, metabolism, and regulation of oxidative stress (Fakhoury, 2018). Accordingly, studies have shown that astrocytes from aged mice are impaired to support neuronal growth and amyloid uptake and clearance, which leads to neurotoxicity accompanied by elevated neuroinflammatory molecules, thus contributing to progressive neuronal loss (Iram et al., 2016; Kovacs, 2020). Chronic neuroinflammation and oxidative stress are observed in tauopathies; astrocytes seem to be involved in both, and TauO accumulation in astrocytes may play a crucial role in these pathological changes (Chun et al., 2020; González-Reyes et al., 2017; Reid et al., 2020).

Cellular senescence is a stress response that has been implicated as a crucial factor in the progression of tau pathology (Bhat et al., 2012; Bussian et al., 2018; Musi et al., 2018). Senescent cells exhibit unique features such as irreversible cell-cycle arrest, resistance to apoptosis, and senescence-associated secretory phenotype (SASP) (Ogrodnik et al., 2019). SASP comprises the active secretion of various inflammatory cytokines, chemokines, and proteases, which serve as an indicator of human aging that actively drives chronic age-related tissue inflammation and degeneration (Bussian et al., 2018). Numerous intracellular and extracellular factors can induce the SASP. A recent study showed that P301S mutant tau-expressing neurons (PS19 mice) induces senescence in glial cells—majorly in astrocytes; these senescent glial cells accumulated in an age-dependent manner and worsened tau pathology through a vicious cycle that drives inflammation, neurodegeneration, and cognitive impairments (Bussian et al., 2018). Further, selective elimination of these senescent cells has shown to prevent the accumulation of pathogenic hyperphosphorylated tau, gliosis, neuronal loss, and restore cognitive functions (Bussian et al., 2018; Musi et al., 2018), indicating that pathological tau-induced cellular senescence and astrocytes dysfunction play a role in the initiation and progression of tau-dependent pathologies (Bussian et al., 2018).

Author Manuscript Author Manuscript Author Manuscript Author Manuscript

Our group has previously shown that TauO co-localizes with astrocytes and microglia in the brain tissues of patients with AD and FTD, and in the retina of tauopathy mice, suggesting their role in triggering chronic neuroinflammation (Nilson et al., 2017). Furthermore, the TauO-associated astrocytes and microglia exhibited relocalization of high mobility group box 1 (HMGB1) from the nucleus to cytoplasm, a molecular signature of senescent cells (Davalos et al., 2013; Jeon et al., 2017; Kim and Davalos, 2019). HMGB1 release is elevated in the brain and CSF of AD patients and aged rodents (Fonken et al., 2016; Fujita et al., 2016; Paudel et al., 2018). HMGB1 is a highly conserved, ubiquitously expressed nuclear protein, which functions to maintain DNA repair, replication, nucleosome structure, and regulation of gene transcription (Lotze and Tracey, 2005). HMGB1-deficient mice die shortly after birth and exhibit severe hypoglycemia, suggesting that HMGB1 is essential for survival (Calogero et al., 1999). Accordingly, loss of nuclear HMGB1 is associated with organ failure, while preserving the nuclear HMGB1 has been shown to improve organ functions and survival (Funayama et al., 2013). Senescent cells actively release HMGB1 into the extracellular environment (Davalos et al., 2013). The extracellular HMGB1 serves as a damage-associated molecular pattern (DAMP), activates receptor for advanced glycation end products (RAGE), and Toll-like receptor 4 (TLR4) on the surface of target cells that promote the expression of inflammatory cytokines such as interleukin-1β (IL-1β), interleukin-6 (IL-6), and tumor necrosis factor α (TNF-α). HMGB1 is a well-established SASP component and serves as a driver of tissue deterioration through senescence-associated inflammation (Basisty et al., 2020; Davalos et al., 2013; Menon et al., 2016; Salminen et al., 2012; Victorelli et al., 2019), and inhibition of HMGB1/SASP could represent a strategy in slowing down aging and related brain pathologies. However, the impact of HMGB1 inhibition on senescent cell load, neuroinflammation, and cognitive impairments in the context of tauopathies has not been investigated.

This study aims to address three key questions: (1) whether TauO associates with senescent astrocytes in the brain of patients with AD and FTD; (2) whether TauO exposure induces HMGB1 release and cellular senescence in cultured astrocytes; and (3) whether inhibition of HMGB1 release by ethyl pyruvate (EP) and glycyrrhizic acid (GA) alleviates tau pathology, cellular senescence, and neuroinflammation in tauopathy mice. This study aims to provide insights into the molecular mechanism of pathological TauO-mediated cellular senescence and neuroinflammation in tauopathy.

RESULTS

TauO-associated astrocytes exhibit a senescence-like phenotype in the brain of patients with AD and FTD

To determine whether TauO are associated with senescent astrocytes in human tauopathy brains, we performed triple-label immunostaining of brain tissue sections from the frontal cortices of patients with AD (n = 8 cases) and FTD (n = 6 cases) and age-matched NDCs, (n = 8 cases) (see Table S1 for the patients demographic and pathological information). As expected, TauO were most abundant in patients with AD and FTD and relatively sparse in the NDCs (Figures 1A–1C). Furthermore, more than 75% of glial fibrillary acidic protein (GFAP)-positive cells (astrocytes) showed immunoreactivity to pathological TauO, and

Author Manuscript Author Manuscript Author Manuscript Author Manuscript

p16^{INK4A} (a robust biomarker of senescence-associated cell-cycle arrest), while a very few TauO-associated GFAP-negative cells were positive for p16^{INK4A} (Figures 1A and 1B). By contrast, significantly fewer TauO- and p16^{INK4A}-positive astrocytes were found in NDC subjects (Figures 1A–1C). Consistent with our previous report (Nilson et al., 2017), we found accumulation of TauO in astrocytes in the frontal cortex of patients with AD and FTD (Figures S1A–S1C). The TauO-associated senescent astrocytes were also confirmed using antibodies against HMGB1, a marker for SASP, and an inflammatory alarmin. We found a significant increase in the TauO-associated astrocytes exhibiting senescent phenotype, as evidenced by elevated cytoplasmic HMGB1 in the brain of patients with AD and FTD (Figures S1D and S1E). Specifically, TauO-associated GFAP-positive astrocytes in AD and FTD brain showed an increased number of γH2AX foci (a marker for senescence-associated DNA damage), and very few γH2AX foci were found in the NDC brain (Figures S1F–S1I). Our results indicate that accumulation of TauO in astrocytes elevated expression of p16^{INK4A}, and γH2AX was accompanied by cytoplasmic HMGB1 translocation; thus, TauO-associated astrocytes predominantly exhibit senescence-like phenotype in the brain of AD and FTD patients.

TauO triggers nucleo-cytoplasmic translocation and release of HMGB1 and mediates senescence-like phenotype in primary astrocytes

Consequent to the above-mentioned observations, we examined whether extracellular TauO are internalized by astrocytes and whether TauO induces HMGB1 release and astrocytes senescence. Therefore, we established primary astrocyte cultures and exposed them to TauO. We found that exogenously provided AF568-labeled TauO were internalized by cultured astrocytes (Figures S2A and S2B). Furthermore, TauO exposure significantly increased the nucleo-cytoplasmic translocation and subsequent release of HMGB1, while in vehicle-treated astrocytes HMGB1 was predominantly located in the nucleus (Figures 2A and 2B). Flow cytometry analysis revealed that upon TauO exposure, more than 70% of the astrocytes were p16^{INK4A} positive (Figure 2C). They also exhibited additional hallmarks of cellular senescence, including increased senescence-associated β-galactosidase (SA-β-gal) activity (Bussian et al., 2018) (Figure 2D; Figures S2C and S2D) and increased G0/G1 cell-cycle arrest (Figure 2E; Figure S2E). Senescent cells are known to accumulate with age and contribute to chronic tissue inflammation and paracrine senescence through their persistent SASP secretion (Acosta et al., 2013). Therefore, we examined whether TauO-induced HMGB1 release/SASP from senescent astrocytes confers senescence to adjacent healthy cells through the paracrine effect. We collected conditional media (CM) from senescent astrocytes and exposed it to healthy astrocytes cultures in the presence or absence of HMGB1 blocking antibody (α-HMGB1). We found that exposure of CM from senescent astrocytes directly promotes senescence-like phenotype in healthy astrocytes, as shown by the increased number of p16^{INK4A}-positive astrocytes (Figure 2F), increased SA-β-gal staining, elevated secretion of SASP factors (IL-6 and TNF-α), and G0/G1 cell-cycle arrest (Figures S2F–S2J). Interestingly, treatment with α-HMGB1 antibody prevented the CM-induced senescence-like phenotype (Figure 2F; Figures S2F–S2J), indicating that HMGB1 released by senescent astrocytes confers senescence to adjacent healthy cells. To test whether extracellular HMGB1 directly promotes astrocyte senescence, we treated primary astrocyte cultures with recombinant HMGB1 (rHMGB1) and measured the SA-β-gal-

Author Manuscript Author Manuscript Author Manuscript Author Manuscript

positive senescent cells. We observed that treatment with rHMGB1 resulted in increased senescence-like phenotype in primary astrocytes as indicated by increased SA-β-gal activity (Figure S2K). These results suggest that direct exposure of TauO drives HMGB1 release and astrocyte senescence, the extracellular HMGB1 and SASP contribute to paracrine senescence, and they also support our finding that TauO-associated astrocytes exhibit a senescence-like phenotype in the brain of AD and FTD patients.

HMGB1 release inhibitors EP and GA prevent TauO-induced senescence-like phenotype in cultured astrocytes

To investigate the role of HMGB1 release in TauO-induced astrocyte senescence, we used EP and GA, the selective and potent inhibitors of HMGB1 release (Mollica et al., 2007; Sun et al., 2018; Ulloa et al., 2002). First, we tested their toxicity on cultured primary astrocytes using lactate dehydrogenase (LDH)-cytotoxicity assay. LDH release analysis showed that both EP and GA were non-toxic to primary astrocytes at the dose used in the study, i.e., 10 mM and 250 μM, respectively (Figure S3A). Next, we investigated the effects of EP and GA on TauO-induced astrocytes senescence and neuroinflammation. Astrocytes were pretreated with EP and GA for 30 min followed by exposure to TauO for 11 days. Flow cytometry analysis showed that both EP and GA significantly decreased the number of $p16^{INK4A}$-positive astrocytes and $p16^{INK4A}$ mean fluorescence intensity (MFI) and inhibited HMGB1 release as shown by increased MFI of intracellular HMGB1 (Figures 3A–3C). Interestingly, a combination of EP and GA showed the maximum decrease in the number of $p16^{INK4A}$-positive astrocytes, $p16^{INK4A}$ MFI, and inhibition of HMGB1 release (Figures 3A–3C). These data were supported by the immunoblot analysis, showing that EP+GA significantly altered the levels of $p16^{INK4A}$ and HMGB1 and its receptor, RAGE (Figures 3D and 3E), and decreased TauO-induced SA-β-gal activity in cultured astrocytes (Figure 3F). We also found that EP+GA attenuated the TauO-induced DNA damage as evidenced by the decreased number of γH2AX foci (Figure S3B), indicating that EP+GA effectively prevents TauO-induced HMGB1 release and limits senescence-associated DNA damage in primary astrocytes. TauO are known to contribute to a vicious cycle of neuroinflammation and subsequent neuronal loss (Nilson et al., 2017). Therefore, we sought to determine the effect of EP and GA on TauO-induced secretion of neuroinflammatory cytokines. Using enzyme-linked immunosorbent assay (ELISA), we found that TauO-stimulated astrocytes had increased secretion of HMGB1, IL-6, and TNF-α, which was significantly reduced by EP +GA (Figures 3G–3I). Various stress-related signaling cascades can trigger cellular senescence and SASP through phosphorylation and activation of the p38-mitogen-activated protein kinase (MAPK) and nuclear factor κB (NF-κB) signaling pathways that coordinate the inflammatory immune responses and are involved in the progressive aging process (Iwasa et al., 2003; Salminen et al., 2012). To determine whether EP and GA inhibit p38-MAPK and NF-κB signaling pathways, we investigated the phosphorylation of p38-MAPK and NF-κB p65 by immunoblotting. We found that EP+GA dose dependently inhibited TauO-induced phosphorylation of p38-MAPK and NF-κB p65 (Figure 3J). EP+GA treatment did not alter total cellular p38-MAPK levels (Figure 3J). These findings suggest that astrocytes undergo TauO-induced senescence via activation of p38-MAPK and NF-κB signaling pathways, and HMGB1 release, a previously unknown pathomechanism that expected to cause a vicious cycle of TauO-induced inflammation, leading to neuronal

Author Manuscript Author Manuscript Author Manuscript Author Manuscript

damage, and thus chronic neuroinflammation. The combination of EP and GA most effectively prevented TauO-induced astrocyte senescence; therefore, EP+GA was used in all subsequent experiments.

Treatment with HMGB1 release inhibitors ameliorates tau pathology and cognitive decline in hTau mice

To examine the role of HMGB1 release in tau pathology *in vivo*, we used hTau transgenic mouse model of tau-dependent neurodegenerative disease, which specifically expresses all six isoforms of human tau protein (Andorfer et al., 2003; Polydoro et al., 2009). At 12 months of age, hTau mice show established tau pathology, NFT deposition, gliosis, neurodegeneration, and cognitive impairments (Andorfer et al., 2003; Polydoro et al., 2009). We sought to determine whether treatment with EP+GA (80 mg/kg + 20 mg/kg) could alleviate TauO pathology and prevent cognitive impairments in hTau mice. Beginning at 12 months of age, male hTau mice were treated with either EP+GA or vehicle, three doses per week for 8 weeks. Hippocampus-dependent spatial memory and exploration potential were examined by Y-maze test immediately before and at the 8-week treatment time points, and mice were also examined in novel-object discrimination tasks at the 8-week treatment (Figure 4A). All the animals were monitored for weight gain/loss during the experiment; no changes were observed (Figure S3C). After the behavior analysis, the mice were euthanized and their brains were processed for immunohistological and biochemical analyses. Thioflavin-S staining of brain sections from hTau mice revealed that treatment of hTau mice with EP+GA significantly reduced NFT deposition in the dentate gyrus (subgranular zone)–the part of the hippocampus where neurogenesis occurs and is associated with memory formation and cognitive functions (Ming and Song, 2011) Figure 4B). Additionally, immunofluorescence staining for phosphorylated tau at S202/T205 in the hippocampus revealed that the inhibition of HMGB1 release by EP+GA treatment attenuated tau phosphorylation at S202/T205, which is relevant for disease-associated tau aggregation (Figure 4C). Compared with vehicle-treated hTau mice, EP+GA-treated hTau mice exhibited significantly enhanced discrimination index, indicating that EP+GA-treated mice had more tendency to explore a novel object than a familiar object (Figure 4D). Furthermore, we found that EP+GA-treated hTau mice performed significantly better in the Y-maze test, indicating that EP+GA treatment significantly alleviates the short-term memory loss in mice with tauopathy (Figure 4E). We also found that neuronal nuclear marker (NeuN)-positive neuronal cells were significantly reduced in vehicle-treated hTau mice, while EP+GA treatment prevented the reduction of NeuN-positive neuronal cells in the CA3 pyramidal layer of hippocampus (Figure 4F) and cortex of hTau mice (Figure S4A). To validate the above-mentioned NeuN immunostaining results, we performed immunoblot analysis of brain homogenates of hTau mice either treated with vehicle or EP+GA and measured the relative expression of NeuN; Postsynaptic density protein 95 (PSD95), a post-synaptic marker; and Synapsin I, a presynaptic marker. Consistent with the above-mentioned NeuN immunostaining results, the immunoblot analysis also indicated significantly reduced protein levels of NeuN, PSD95, and Synapsin I in the vehicle-treated hTau mice, which was prevented in EP+GA-treated hTau mice (Figure S4B). Thus, these results suggest that HMGB1 release plays a key role in tau-dependent pathologies and cognitive impairments.

Author Manuscript Author Manuscript Author Manuscript Author Manuscript

Treatment with HMGB1 release inhibitors modulates senescent cells in 12-month-old hTau mice

We investigated whether the EP+GA treatment results in decreased senescence in the brain of hTau mice. Immunofluorescence microscopy analysis revealed that TauO-associated $p16^{INK4A}$ expression was significantly reduced in the hTau mice that received the EP+GA treatment compared with the vehicle-treated hTau mice (Figures 5A–5C). We observed that EP+GA reduced the number of $p16^{INK4A}$-positive astrocytes in the brain of hTau mice (Figures S4C–S4E). EP+GA treatment greatly reduced TauO load (Figure 5C) and the MFI of $p16^{INK4A}$ (Figure 5D) and decreased the number of TauO-associated GFAP- and $p16^{INK4A}$-positive senescent-like cells (Figure 5E). Furthermore, using immunoblot analysis of brain homogenates, we validated that protein levels of TauO, γH2AX, and $p16^{INK4A}$ were significantly decreased in the brain of EP+GA-treated hTau mice compared with vehicle-treated hTau mice (Figures S4F and S4G). Increased GFAP expression–an indicator of astrogliosis–has been closely associated with astrocyte senescence both *in vitro* and *in vivo* (Boisvert et al., 2018; Lye et al., 2019). GFAP levels increase during tau pathology and aging that correlates with cognitive impairment in AD patients (Cohen and Torres, 2019; Oeckl et al., 2019); therefore, we measured GFAP fluorescence intensities in the brain of vehicle-treated and EP+GA-treated hTau mice. We found that GFAP expression was markedly decreased in the brain of EP+GA-treated hTau mice, indicating EP+GA treatment inhibited astrogliosis (Figure S4H). Furthermore, we confirm that cytoplasmic HMGB1-positive cells were significantly decreased in the brain of EP+GA-treated hTau mice (Figures 5F and 5J). Additionally, EP+GA treatment reduced the number of γH2AX foci (Figures 5G and 5K), $p16^{INK4A}$-positive cells (Figures 5H and 5L), and IL-6-positive cells in the brain of hTau mice (Figures 5I and 5M). Consistent with the reduction of TauO and senescent cells observed during EP+GA treatment, the concentrations of the neuroinflammatory cytokines IL-6 and TNF-α were significantly reduced in the hippocampus and cortex of EP+GA-treated hTau mice compared with vehicle-treated control mice (Figures S5A and S5B). The circulating HMGB1 levels in the serum and those of its receptor, RAGE, in the brain were also significantly decreased in EP+GA-treated hTau mice (Figures S5C and S5D). Polydoro et al. (2009) demonstrated that compared with wild-type control mice, hTau mice exhibit remarkable age-dependent tau pathology and cognitive and physiological impairments. In our previous study, we reported the increased nucleo-cytoplasmic translocation of HMGB1 in hTau mice was accompanied with elevated levels of TauO, while HMGB1 was abundantly localized in the nucleus in wild-type mice with negligible levels of TauO (Nilson et al., 2017). The HMGB1 nucleo-cytoplasmic translocation and its subsequent release are consistent during senescent phenotype, neuroinflammatory responses, and cognitive dysfunctions (Aucott et al., 2018; Davalos et al., 2013; Paudel et al., 2018). To confirm the observed benefits of EP+GA treatment on hTau mice were due to tau pathology/senescence, we determined the impact of HMGB1 release inhibition on wild-type control mice. We found no statistical differences in vehicle-treated or EP+GA-treated mice in terms of protein levels of senescence markers γH2AX and HMGB1, while RAGE expression was decreased by EP+GA treatment (Figures S5E and S5F). Additionally, no significant changes were found in Y-maze spontaneous alternation test (Figure S5G) and novel-object recognition (NOR) task in vehicle-treated or EP+GA-treated wild-type mice (Figures S5H and S5I), suggesting that EP+GA treatment shows specific protective effects in aged hTau mice.

Author Manuscript Author Manuscript Author Manuscript Author Manuscript

Collectively, these results indicate that TauO-associated senescent-like cells and HMGB1 release play a crucial role in TauO pathology.

DISCUSSION

Pathological TauO triggers chronic neuroinflammation during AD, FTD, and many other tauopathies (Guzman-Martinez et al., 2019; Nilson et al., 2017; Reid et al., 2020), and TauO accumulation in astrocytes may play a crucial role in pathological events (Chun et al., 2020; González-Reyes et al., 2017; Reid et al., 2020). The effect of TauO on astrocytes and the underlying mechanism for TauO-induced aging-related neuroinflammation are still unknown. In the present study, we report that (1) TauO-associated astrocytes exhibit markers of senescence-associated cell-cycle arrest ($p16^{INK4A}$), senescence-associated DNA damage (γH2Ax foci), and SASP (HMGB1) in the brains of patients with AD and FTD; (2) direct exposure of TauO triggers cellular senescence in cultured astrocytes; (3) HMGB1 release is a crucial event during TauO-induced senescence in cultured astrocytes; (4) the extracellular HMGB1 induces paracrine senescence in neighboring healthy astrocytes; (5) treatment with HMGB1 release inhibitors (EP+GA) prevents activation of p38-MAPK and NF-κB signaling pathways and reduces levels of TauO-associated SASP and neuroinflammation; (6) *in vivo* long-term (8-week) treatment with EP+GA prevents astrogliosis and neuroinflammation and reduces levels of TauO, hyperphosphorylated tau, and NFT deposition; and (7) treatment with EP+GA significantly reduces the number of senescent-like cells in the brains of hTau mice, thus preventing learning and memory impairments. These findings suggest that HMGB1–a SASP factor–plays a crucial role during TauO-induced cellular senescence and cognitive decline in tauopathies. This study also revealed that inhibition of HMGB1 release by EP+GA is effective in delaying the disease onset in hTau mice. This study importantly contributes to illustrating the molecular events underlying aging-related tauopathies, emphasizing the role of TauO-induced astrocyte senescence, HMGB1 release, and subsequent paracrine senescence and neuropathology in AD and FTD. This work substantially advances our knowledge on the role of HMGB1 release in TauO-induced cellular senescence and chronic neuroinflammation in tauopathies, and targeting HMGB1 release may lead to development of therapeutic approaches that halt the progression of tauopathies.

The role of astrocyte senescence in tauopathies is complicated and unresolved. Astrocyte activation is involved in multiple brain pathologies. However, astrocytes senescence was shown to contribute in tauopathy by releasing a plethora of pro-inflammatory and cytotoxic factors (Bussian et al., 2018). Here, we found that TauO-associated senescent astrocytes were highly abundant in the brain tissues of patients with AD and FTD. Our findings provide complementary insights for the studies showing astrocyte senescence as a component of AD, and elimination of senescent glial cells prevent tau pathology and cognitive dysfunction (Bussian et al., 2018; Musi et al., 2018). The emerging evidence suggests that senescent glial cells contribute to the initiation and progression of neurodegeneration and cognitive dysfunction in AD and FTD (Bussian et al., 2018; Clarke et al., 2018; Cohen and Torres, 2019; Limbad et al., 2020; Salminen et al., 2011). Extracellular TauO are rapidly internalized and abundantly accumulated by astrocytes that promote synaptic dysfunction via reduced gliotransmitter availability and contribute to tau pathology

Author Manuscript Author Manuscript Author Manuscript Author Manuscript

propagation (Piacentini et al., 2017). A recent study demonstrated that the low-density lipoprotein-related protein 1 (LRP1) is a master regulator of tau internalization by neurons (Rauch et al., 2020), but LRP1 is highly expressed in reactive astrocytes in AD (Arèlin et al., 2002). Indeed, neuronal-specific knockdown of LRP1 decreased transsynaptic tau propagation, but increased tau accumulation in astrocytes (Rauch et al., 2020). Furthermore, tau accumulation in astrocytes effectively induces neuronal dysfunction and memory deficits in mice (Richetin et al., 2020), and astrocytic tau accumulation was also observed in the brain of patients with tauopathies (Chin and Goldman, 1996; Gomez-Tortosa et al., 2019; Kovacs, 2020; Kovacs et al., 2016, 2017b; Nolan et al., 2019), suggesting tau accumulation in astrocytes might contribute to dementia in patients with tauopathies. Importantly, astrocytes are very sensitive to senescence-inducing stimuli (Bitto et al., 2010), indicating that astrocyte senescence is more abundant in the brain (Bitto et al., 2010; Bussian et al., 2018; Chinta et al., 2018; Cohen and Torres, 2019; Han et al., 2020; Limbad et al., 2020). Therefore, understanding the mechanisms by which TauO induces senescence in astrocytes is of interest to this study.

Accumulation of the pathological tau in astrocytes increases with age in mice expressing P301L tau, which consequently promotes neurodegeneration even in the absence of neuronal tau inclusions (Forman et al., 2005). The pathological TauO might cause astrocytic dysfunctions via cellular senescence. Astrocytic dysfunction and gain of SASP could promote neuronal degeneration through increased disruption of the blood-brain barrier (Forman et al., 2005; Heithoff et al., 2021), resulting in neurotoxicity mainly due to the loss of their neurotrophic effects and gain of toxic functions (Perez-Nievas and Serrano-Pozo, 2018). However, the special relationship between pathological tau and astrocytes has received less attention not only in AD but also in all human tauopathies, including FTD, corticobasal degeneration, progressive supranuclear palsy, Pick disease, chronic traumatic encephalopathy, or argyrophilic grain disease.

We observed that when cultured astrocytes were exposed to TauO, most of them displayed features of cellular senescence, suggesting that pathogenic TauO exposure is sufficient to trigger astrocyte senescence. It is well known that senescent cells substantially contribute to inflammation, tissue deterioration, and physical dysfunction through SASP (Xu et al., 2018). Extracellular HMGB1 serves as a major inflammatory SASP component that has been shown to play a critical role during the initiation and spread of cellular senescence and contributes to the vicious cycle of chronic inflammation (Davalos et al., 2013; Jeon et al., 2017; Kim and Davalos, 2019; Nilson et al., 2017). Therefore, we examined the role of extracellular HMGB1 in TauO-induced cellular senescence. Our data indicated that inhibition of HMGB1 release by EP+GA effectively limits the expression of senescence markers in astrocytes. Additionally, neutralization of extracellular HMGB1 by α-HMGB1 antibody in CM from senescent astrocytes prevented the paracrine senescence in healthy adjacent astrocytes, suggesting HMGB1 release is an important event during TauO-induced astrocyte senescence and neuropathology. Pieces of evidence support the notion that targeting senescent cells and SASP provides benefits in ameliorating AD and FTD pathologies in the mouse models (Bussian et al., 2018; Musi et al., 2018; Zhang et al., 2019a). The clinical relevance of our observation is also supported by evidence that shows HMGB1 is increased in CSF of AD patients, which strongly correlates with the rapid

Author Manuscript Author Manuscript Author Manuscript Author Manuscript

progression of dementia (Fujita et al., 2016; Paudel et al., 2020). Using EP and GA–the specific inhibitors of HMGB1 release–we showed that HMGB1 release is a key event during TauO-induced astrocytes senescence and inflammation. We found that EP+GA inhibited TauO-induced activation of p38-MAPK and NF-κB signaling pathways–the critical regulators of the SASP that activated by various intracellular and extracellular stressors (Freund et al., 2011). These findings suggest that EP+GA not only prevents HMGB1 release but also inhibits astrocyte senescence through inhibition of SASP (Iwasa et al., 2003; Salminen et al., 2012). Importantly, EP+GA treatment for 8 weeks decreased inflammation in the brain as well as in circulation in aged, tauopathy mice. Our findings are in accordance of the study demonstrating that inhibition of p38-MAPK in both pre-senescent and senescent human astrocytes limits the upregulated level of SASP factors (Bhat et al., 2012).

Our data show that EP+GA-treatment for 8 weeks decreased the number of TauO-associated senescent cells in the brain of aged, tauopathy mice. Consistent with this observation, EP +GA treatment also decreased levels of pro-inflammatory cytokines in both brain and serum, which may be due, in part, to the inhibition of HMGB1 release/SASP. However, direct anti-inflammatory activities of EP and/or GA on astrocytes and microglia are also possible. It is noteworthy that inhibiting HMGB1 release by EP and GA is identified as experimental therapeutics that significantly protect animals against ischemia, lethal sepsis, hepatitis, hemorrhagic shock, brain injury, and inflammation (Fink, 2007; Mollica et al., 2007; Shen et al., 2010; Tang et al., 2020; Ulloa et al., 2002; Wang et al., 2007; Zhao et al., 2017). Both the HMGB1 release inhibitors have been examined in humans and shown to be safe at clinically relevant doses (Bennett-Guerrero et al., 2009; Chen et al., 2019; Fink, 2007; Kwon et al., 2020). However, future work is required to investigate how EP and GA prevent TauO-induced HMGB1 release and cellular senescence. One possible mechanism is that the EP and GA upregulate Sirtuin 1-NAD^+-dependent deacetylases, which is known to inhibit the acetylation and release of HMGB1, cellular senescence, and aging (Hou et al., 2017; Kim et al., 2016; Lee et al., 2019; Satoh et al., 2013).

Using the Y-maze test and NOR test, we examined hippocampus-dependent learning and memory. We report that 8-week treatment with EP+GA improved cognitive functions in hTau tauopathy mice. These beneficial effects of EP+GA treatment were associated with decreased levels of TauO, hyperphosphorylated tau, NFT deposition, and attenuated neuroinflammation. Our findings are supported by a recent work that showed targeting HMGB1 by EP alleviates systemic lupus erythematosus and reversed the senescent phenotype in bone-marrow-mesenchymal stem cells (Zhang et al., 2019b). Human primary astrocytes have been shown to undergo cellular senescence and produce SASP factors (Limbad et al., 2020). Senescence induction in astrocytes leads to impaired glutamate homeostasis, and CM from the senescent astrocytes causes toxicity to cortical neurons (Limbad et al., 2020). HMGB1 stimulation induces senescence-related transcriptomic alternations and perpetuates neuroinflammation, and functional inhibition of HMGB1 prevents most of the senescence-associated changes (Nicaise et al., 2019). Consistent with our findings, a study has shown that anti-HMGBI antibody therapy improved cognitive functions and decreased γH2AX levels in an AD mouse model (Fujita et al., 2016). Thus, inhibition of HMGB1 release is a potentially promising strategy for alleviating aging-associated tauopathies.

Author Manuscript Author Manuscript Author Manuscript Author Manuscript

In summary, our findings reveal that extracellular HMGB1 plays a key role in TauO-induced cellular senescence, chronic neuroinflammation, and progression of aging-related tau pathology. TauO-induced HMGB1 release could represent an important common pathomechanism in tauopathies including AD and FTD. EP and GA are potent inhibitors of TauO-induced HMGB1 release, which prevents cellular senescence and neuroinflammation in astrocyte cultures as well as in an *in vivo* model of tauopathy. This study describes a strategy to prevent TauO-associated senescence and inflammation using EP+GA. The effects of EP and GA on improved cognitive functions result solely from the inhibition of HMGB1/SASP or also involve indirect actions on neuronal and glial cell functional state, and potential senolytic action of EP+GA remains to be investigated. However, our findings pave the way for future research that will test the hypothesis that targeting TauO-induced HMGB1-SASP can suppress neuropathology and preserve cognitive functions in aging-related neurodegenerative disorders such as AD and FTD and many other tauopathies.

STAR★METHODS

RESOURCE AVAILABILITY

Lead contact—Further information and requests for resources and reagents should be directed to and will be fulfilled by the Lead Contact, Prof. Rakez Kayed (rakayed@utmb.edu).

Materials availability—This study did not generate new unique reagents.

Data and code availability

- Original full Immunoblot images have been deposited at Mendeley data and are publicly available as of the date of publication. The DOI (https://dx.doi.org/10.17632/765jbfjc5k.1) is listed in the Key resources table. Microscopy data reported in this paper will be shared by the lead contact upon request.
- This study does not generate or utilize any computer codes or algorithms.
- Any additional information required to reanalyze the data reported in this paper is available from the lead contact upon request.

EXPERIMENTAL MODEL AND SUBJECT DETAILS

Mice—hTau mice (stock #004808) and C57BL/6J mice (stock#000664) were purchased from The Jackson Laboratory and maintained at the University of Texas Medical Branch (UTMB) animal facility. All the offsprings were genotyped by PCR analysis using DNA extracted from ear-punch tissues. hTau mice express all the six isoforms of human tau protein but do not express mouse tau (Polydoro et al., 2009). The hTau mice develop age-dependent tau pathology. At 12-months of age, these mice show impaired cognitive and synaptic functions and established tauopathy (Polydoro et al., 2009). Beginning at 12-months of age, male hTau mice and C57BL/6J mice were randomly assigned to the control or treatment group. Mice were injected intraperitoneally (i.p.) either with saline (vehicle) or HMGB1 inhibitors, ethyl pyruvate (PubChem ID: 12041; 80 mg/kg bodyweight; Sigma#8066170100) and glycyrrhizic acid or glycyrrhizin (PubChem ID: 14982; 20 mg/kg

Author Manuscript Author Manuscript Author Manuscript Author Manuscript

bodyweight; Sigma#50531) in 0.4 mL saline for 8-weeks (3-doses per week) beginning at 12-months age. Mice were housed in a 12h:12h light: dark cycle and pathogen-free conditioning cages with free access to water and food. All the animals were monitored for weight gain/loss, grooming changes, and posture during the experiment, and no changes were observed. After the treatment, the animals were examined for cognitive function and neuropathology. All animal experiments were performed in compliance with the National Institute of Health Guidelines under protocols approved by the Institutional Animal Care and Use Committee at the University of Texas Medical Branch, Galveston.

Primary astrocytes culture—Primary astrocyte cultures were prepared from mixed glial cultures as described by McCarthy and de Vellis (1980) and Schildge et al. (2013). Briefly, C57BL/6 wild-type pups (P0-P3) were euthanized, and brain tissues were isolated. The cerebellum and meninges were removed using forceps under the dissection scope. The cleaned cerebral tissues (4 brains) were pooled together in ice-cold Hank's balanced salt solution (HBSS, GIBCO #14175-095), and tissues were minced using forceps and dissociated in 0.25% trypsin in HBSS at 37°C for 30 min with frequent shaking. FBS (10%) and DNase I (1 mg/ml) were added, samples were placed on ice for 5 minutes to halt the trypsinization. Samples were centrifuged at 300 g for 5 minutes at 25°C, and supernatants were discarded, and the pellet was resuspended in HBSS and triturated using 1 mL pipette. To remove large debris, the sample tubes were kept in an upright position for 5 minutes, and then samples were transferred to fresh tubes and centrifuged at 300 g for 8 minutes at 25°C. The cell pellet was resuspended in glial cell culture media containing DMEM (GIBCO) with FBS (10%), Antibiotic-Antimycotic (1X). Cells were counted, and 10 million cells were plated on a poly-L-lysine (PLL) coated T75 flask in glial cell culture media for 12-14 days in a humidified incubator (37°C, 5% CO_2, and 95% air), with media changes after every 4-5 days. Unwanted glial cells were removed by the shake-off method, purity of adherent astrocytes was determined by GFAP immunostaining, we found that the purity of the astrocytes culture was > 90%, were used for the experiments (Figure S5J).

METHOD DETAILS

Immunofluorescence staining—Mice were transcardially perfused; brains were isolated and fixed in 4% paraformaldehyde in PBS at 4°C for 24h, followed by cryoprotection in 30% (w/v) sucrose in PBS for 2-3 days at 4°C. Brain sections (12μm) were made on a freezing microtome and used for immunofluorescence studies. Frontal cortices of frozen brain tissues from AD patients (N = 8 cases), FTD patients (N = 6 cases), and age-matched non-demented control (NDC) subjects (N = 8 cases) were received as frozen blocks from the Institute for Brain Aging and Dementia at UC Irvine and approved by the Institutional Ethics Committee. Immunofluorescence was performed as previously described (Farmer et al., 2020; Montalbano et al., 2020). Briefly, the sections were fixed in ice-chilled methanol for 20 min and treated with TrueBlack Lipofuscin Autofluorescence Quencher for 15 min (Biotium #23007). After washing in PBS, the sections were blocked for 1h with 5% goat serum and 5% bovine serum albumin (BSA) in PBS and incubated with rabbit-anti-human $p16^{INK4A}$ (D3W8G antibody, for human tissues) (1:100; CST #92803) or rabbit anti-mouse $p16^{INK4A}$ (M-156 antibody, for murine tissues) (1:100; #SC-1207) or anti-HMGB1 antibody (1:100; #ab18256) or anti-γH2AX antibody (1:100; CST #9718) (1:100), mouse-

Author Manuscript Author Manuscript Author Manuscript Author Manuscript

anti-TauO-specific monoclonal antibody clone 2 (TOMA) (1:100) (Montalbano et al., 2020) and chicken-anti-GFAP antibody (1:500; #ab4674) (1:500), AT8 antibody (1:100; Thermo #MN1020), anti-IL6 antibody (1:200; CST #12912) or recombinant Alexa fluor488 anti-NeuN antibody (1:250; # ab190195) in antibody diluent at 4°C overnight. After washing with PBS, the sections were incubated with or without anti-rabbit IgG Alexa flour-568, anti-mouse IgG Alexa flour-633, and anti-chicken IgG Alexa flour-488 (1:500, Invitrogen, Waltham, MA) for 1 h at room temperature. The sections were mounted with ProLong Gold Antifade reagent with DAPI (Thermo#P36935) and imaged on a fluorescence microscope (Keyence BZ-X710, USA) and analyzed with ImageJ (NIH, Bethesda) and BZ-X Analyzer (Keyence, USA).

Monolayer cultures of primary astrocytes were fixed in 4% paraformaldehyde (Sigma# F8775) and permeabilized with PBS containing 0.25% Triton X-100 for 10 minutes. After washing with PBS, the cells were blocked in PBS containing (5% goat serum, 5% BSA) for 30 minutes at room temperature. Cells were then incubated with primary antibodies against HMGB1 (1:500), $p16^{INK4A}$ (1:500), overnight at 4°C. After three washes with PBS, the cells were incubated with goat anti-rabbit IgG conjugated with Alexa Flour 568 (1:500, Invitrogen) for 30 minutes at room temperature. Following three washes, the slips were mounted on slides with anti-fade mounting media containing DAPI as nuclear counterstaining. Nuclear HMGB1 and DAPI positive (total cells) were counted in ten random fields per sample to determine the percentage of cytoplasmic HMGB1 or $p16^{INK4A}$ positive cells.

TauO production and treatment—For the exogenous treatment, TauO have been produced and characterized by established protocols (Ghag et al., 2018; Ising et al., 2019; Puangmalai et al., 2020). Briefly, human wild-type 2N4R tau-expressing, isopropyl β-D-thiogalactopyranoside (IPTG) inducible plasmid was transformed into *Escherichia coli* BL21(DE3) competent cells (Agilent# 200131). A single colony was selected and grown at 37°C with continuous shaking (180 rpm) until the culture reached OD_{600} = 0.4-0.6; then human tau expression was induced by the addition of IPTG (0.5mM) for 3h. After induction, cells were centrifuged at 10,000xg for 10 min, the pellets were resuspended in Brinkley Renaturing Buffer 80 (BRB-80) containing PIPES 80 mM, magnesium sulfate 1 mM, EGTA 1 mM at pH 6.8 supplemented with 2-mercaptoethanol (0.1%), and PMSF (1 mM). The resuspension was sonicated for 4-5 cycles of 30 s bursts on ice, followed by centrifugation at 10,000xg for 10 min to remove the bacterial debris. The tau-containing supernatants were boiled for 10 min, centrifuged again, and were applied to a cation exchange chromatography column (Cytiva# 29018183). Tau was eluted with increasing concentrations of sodium chloride dissolved, and the elution fractions were collected and examined for the presence of tau by a Coomassie staining of protein gel. Tau-containing fractions were combined and purified further using size exclusion chromatography (Superdex 200 Increase 10/300 GL, Cytiva# 28990944). The eluted fractions were analyzed by a silver staining of protein gel and the purest tau-containing fractions were combined. Buffer replacement was carried out several times to remove all remaining endotoxins and degraded tau protein. The final concentrated tau protein was collected from the columns and normalized to 1 mg/ml using the BCA assay. The tau protein was aliquoted and lyophilized and stored at −80°C. Tau

Author Manuscript Author Manuscript Author Manuscript Author Manuscript

protein was resuspended in PBS and TauO was prepared as described earlier (Gerson et al., 2017; Lasagna-Reeves et al., 2010). The astrocytes were pretreated with or without EP+GA for 30 min at indicated concentrations then stimulated with TauO for 11-days at 37°C and 5% CO2 in humidified incubators. After media removal, the cells were analyzed for biomarkers of senescence by immunofluorescence assays, flow cytometry, and western blot. For internalization experiments, TauO were labeled using AF568 protein labeling kit (Invitrogen# A10238) as described previously (Puangmalai et al., 2020). Primary astrocytes were incubated with or without AF568-labeled TauO for 3h. After incubation, extracellular TauO was removed by three washes with PBS followed by immunostaining for GFAP and DAPI and examined under a fluorescence microscope (Keyence BZ-X710).

Senescence-associated β-galactosidase assay—SA-β-gal staining was performed using a Cellular Senescence Assay kit (Sigma #KAA002) as per the manufacturer's instructions, and dark blue-stained cells were counted as senescent cells under Keyence BZ-X710 microscope. Total cells were counted using a nuclear fast red or DAPI counterstaining in ten random fields per sample to determine the percentage of SA-β-gal positive cells.

Treatment with conditional media and rHMGB1—Primary astrocytes were cultured in presence of TauO (0.5 μM) for 11-days, conditional media (CM) were collected, and spun down to remove cellular debris, and then frozen at −80°C. For HMGB1 blocking antibody experiments, CM was incubated with or without 4 μg/ml α-HMGB1 antibody for 1 h at 37°C. The CM were then applied to fresh astrocytes cultures for 4-days, and senescence was assayed. In parallel experiments, to determine the effect of extracellular HMGB1 on astrocyte senescence, we used recombinant HMGB1 (rHMGB1) that was a kind gift from Professor Junji Iwahara (Zandarashvili et al., 2013). Astrocyte cultures were treated with rHMGB1 (1 μg/ml) for 4-days and senescence was assayed.

Flow cytometry analysis—Astrocytes cultured in a 6-well plate were pretreated with either ethyl pyruvate (10 mM) or GA (250 μM) followed by stimulation with or without TauO at a concentration of 0.5 μM. After 11-days, cells were washed with Hank's balanced salt solution followed by trypsinization and collected via centrifugation at 300 g for 10 min and resuspended in flow cytometry buffer (HBSS with 1% fetal bovine serum (GIBCO) and 1 mM EDTA (Sigma). Cells were fixed in ice-chilled methanol for 10 min followed by washing and blocking, cells were stained with primary antibody anti-mouse $p16^{INK4A}$ (1:100) or anti-HMGB1 antibody for 30 min on ice. After 3-washes, cells were stained with anti-rabbit AF488 (1:500) for 15 min on ice followed by four washes. To quantify $p16^{INK4A}$ positive senescent cells and intracellular HMGB1 levels, 10,000 cells from each group were counted, gated for viable and singlet cells, and determined the percentage of $p16^{INK4A}$+ senescent cells, $p16^{INK4A}$ median fluorescence intensity (MFI) and MFI of intracellular HMGB1 using LSRII Fortessa Analyzer (BD Biosciences). Each experiment was conducted a minimum of three times, and data from each experiment were combined for analysis and bar graphs. In parallel experiments, cell cycle analysis was performed using FxCycle™PI/RNase staining solution (Invitrogen, #F10797) as per the manufacturer's instructions.

Author Manuscript Author Manuscript Author Manuscript Author Manuscript

Immunoblotting—Relative protein levels were measured by immunoblotting, as described previously (Puangmalai et al., 2020). Briefly, mouse brains were homogenized at 50 pulses/sec for 30 s using TissueLyser LT (QIAGEN) in PBS containing 2% protease/phosphatase inhibitors cocktail (Sigma; Cat#p8340) at 1:3 ratio brain:PBS (w/v). Samples were centrifuged at 10,000 g for 10 min at 4°C and supernatants were collected and stored in aliquots at −80°C until used for immunoblotting. Cell lysates were prepared in ice-cold RIPA buffer (CST; #9806) containing 2% protease/phosphatase inhibitors cocktail (Sigma; #p8340). After centrifugation for 10 min at 13,000 g and 4°C, the supernatant was collected and quantified using the PierceTM BCA protein assay kit (Thermo; #23225). An equal amount of protein (10 μg) from each sample was loaded in Pre-cast NuPAGE 4%–12% Bis-Tris Gels, run under reducing conditions, followed by transfer to nitrocellulose membranes. After blocking for 1 h at RT with 10% nonfat dried milk, membranes were probed with anti-$p16^{INK4A}$ antibody (1:1000, #sc-1207), anti-HMGB1 antibody (1:1000, abcam #ab18256), ant-RAGE antibody (1:1000, abcam #ab37647), anti-phospho-p38 MAPK (1:1000, CST #9216), anti-total p38 MAPK (1: 1000, CST #9212), anti-phospo-NF-κB p65 (1:1000, CST #3033), T22 TauO-specific antibody (1:500) (Nilson et al., 2017), anti-γH2AX antibody (CST #9718), NeuN antibody (Chemicon #MAB377), anti-PSD95 antibody (abcam #ab18258), and anti-synapsin I antibody (abcam #ab8). Anti-GAPDH antibody (1:25000, abcam #ab9485) or monoclonal Anti-β-Actin–Peroxidase antibody (1: 25000, Sigma #A3854) was used as a loading control, and for immunoreactivity detection horseradish peroxidase (HRP)-conjugated anti-rabbit or anti-mouse IgG (1:10,000, GE Healthcare) were used. WesternBright ECL HRP substrate (Advanstra #K-12045-D50) was used to develop the signal, and ImageJ (NIH) was used for densitometry analysis and normalized against respective loading controls. Sources, specificity, and identifier of antibodies used in this study are provided in the Key resources table.

Novel-object recognition (NOR) and Y-Maze Test—Following 8-weeks of HMGB1 inhibitors treatment, all the mice were subjected to cognitive evaluation in the NOR and Y-Maze Tests. NOR testing performed to measure the memory deficits in hTau mice, as described previously (Gerson et al., 2016; Polydoro et al., 2009). Briefly, at day-1 from each group, mice were acclimatized to the NOR arena (white open-field, 60 cm height, and 55 cm in diameter) for 15 min. On day 2, mice were familiarized with two identical objects for 15 min. On day three, mice were tested for 15 min with one familiar object (presented during familiarization) and one novel object (different in shape and color, but sharing a common size and volume). After each trial, the apparatus cleaned with 70% ethanol. Time spent exploring each object was recorded using ANY-Maze software. Differences in learning and memory of the mice were expressed as a discrimination index and novelty preference, calculated by given following formula: *Discrimination index* = (T (Novel) – T (familiar))/(T (Novel) + T (familiar).

Y-maze test was used to evaluate short-term working memory, as described previously (Gerson et al., 2016). Briefly, After completion of the 8-weeks treatment, mice (n = 5–6 per group) were placed at the center of the Y-maze (San Diego Instruments, San Diego, CA) and allowed to explore for one 8-min trial. The total number of arm entries and sequences of arm entries were recorded. One successful spontaneous alternation recorded when an animal

Author Manuscript Author Manuscript Author Manuscript Author Manuscript

consecutively enters three different arms of the maze and the percent spontaneous alternation over an 8-min trial calculated using the following formula.

$$\%\ spontaneous\ alternation = (\#\ spontaneous\ alterations)/(\text{total number of arm entries} - 2) \times 100$$

NFTs staining—NFTs in the hTau mice brain were stained and quantified with classic thioflavine-S staining (Bussian et al., 2018; Ly et al., 2011). Briefly, brain sections on glass slides were washed in 70% ethanol for 1 min and 80% ethanol for 1 min. Sections were incubated for 15 min at room temperature in 1% thioflavin-S (Sigma# T1892) solution in 80% ethanol (0.2 μM filtered). Slides were then washed with 80% ethanol for 1 min, 70% ethanol for 1 min, followed by two washes with double distilled water. Then, the sections were mounted with a coverslip using anti-fade mounting media containing DAPI. The NFTs were visualized under the fluorescence microscope and quantified using BZ-X-analyzer (Keyence, USA).

Cytokine measurements—Secretory levels of IL-6 (Thermo Cat#88-7064), TNF-α (Thermo Cat#88-7324), and HMGB1 (Novus Biologicals Cat#NBP2-62766) in the culture supernatants and brain homogenates were measured by ELISA kits as per the manufacturer's instructions. Briefly, ELISA plates were coated with capture antibody in coating buffer (either IL-6, TNF-α, or HMGB1) 100 μL/well and incubated overnight at 4°C. The wells were washed 3 times with washing buffer (1x PBS, 0.05% Tween-20, 250μL/well), the plate was blotted on absorbent paper to remove the residual buffer and blocked for 1 hour with 1X Assay Diluent or 1% bovine serum albumin (BSA, 200 μL/well) at room temperature. After 3 washes, samples or standards (100 μL/well) were added and the plate was incubated overnight at 4°C. This was followed by 4 washes, and the addition of detection antibody in 1X assay diluent or 1% BSA (biotin-labeled anti-cytokine antibody either IL-6, TNF-α, or HMGB1) for 1 hour at room temperature. The wells were washed 5-6 times and Avidin-HRP diluted in 1X assay diluent or 1% BSA was added and incubated for 30-45 minutes at room temperature. Then the wells were washed 7 times and substrate solution (100 μL/well) was added. The plates were incubated at room temperature for 15-20 minutes to allow the development of blue color; then the reaction was terminated by the addition of stop solution (50 μL/well). The plate was read at 450nm using an ELISA reader and the values of standards were plotted (OD_{450} versus concentration) and the cytokine concentration in samples was estimated from the standard curve.

QUANTIFICATION AND STATISTICAL ANALYSIS

All *in vitro* experiments were performed in at least three biological replicates. All data are presented as means ± SEM and were analyzed using GraphPad Prism 6. Statistical analyses included the Student t test or one-way ANOVA followed by Tukey's multiple comparisons test. Column means were compared using one-way ANOVA with treatment as the independent variable. Additionally, group means were compared using a two-way ANOVA with factors on treatment, respectively. When ANOVA showed a significant difference, pairwise comparisons between group means were examined by Tukey's multiple comparison

Author Manuscript Author Manuscript Author Manuscript Author Manuscript

tests. Differences were considered statistically significant if a p value less than 0.05. Details of statistical analysis can be found in respective figure legends.

Supplementary Material

Refer to Web version on PubMed Central for supplementary material.

ACKNOWLEDGMENTS

We thank Professor Junji Iwahara (UTMB) for providing the rHMGB1 protein. This work was supported by the Mitchell Center for Neurodegenerative Diseases; the National Institutes of Health grants R01AG054025, R01NS094557, RFA1AG055771,and R01AG060718; and the American Heart Association collaborative grant 17CSA33620007 (to R.K.); U.S. supported by T32 AG058522.

REFERENCES

Acosta JC, Banito A, Wuestefeld T, Georgilis A, Janich P, Morton JP, Athineos D, Kang TW, Lasitschka F, Andrulis M, et al. (2013). A complex secretory program orchestrated by the inflammasome controls paracrine senescence. Nat. Cell Biol 15, 978–990. [PubMed: 23770676]

Andorfer C, Kress Y, Espinoza M, de Silva R, Tucker KL, Barde YA, Duff K, and Davies P (2003). Hyperphosphorylation and aggregation of tau in mice expressing normal human tau isoforms. J. Neurochem 86, 582–590. [PubMed: 12859672]

Andreasen N, Minthon L, Davidsson P, Vanmechelen E, Vanderstichele H, Winblad B, and Blennow K (2001). Evaluation of CSF-tau and CSF-Abeta42 as diagnostic markers for Alzheimer disease in clinical practice. Arch. Neurol 58, 373–379. [PubMed: 11255440]

Arélin K, Kinoshita A, Whelan CM, Irizarry MC, Rebeck GW, Strickland DK, and Hyman BT (2002). LRP and senile plaques in Alzheimer's disease: colocalization with apolipoprotein E and with activated astrocytes. Brain Res. Mol. Brain Res 104, 38–46. [PubMed: 12117549]

Aucott H, Lundberg J, Salo H, Klevenvall L, Damberg P, Ottosson L, Andersson U, Holmin S, and Erlandsson Harris H (2018). Neuroinflammation in Response to Intracerebral Injections of Different HMGB1 Redox Isoforms. J Innate Immun 10, 215–227. [PubMed: 29478057]

Basisty N, Kale A, Jeon OH, Kuehnemann C, Payne T, Rao C, Holtz A, Shah S, Sharma V, Ferrucci L, et al. (2020). A proteomic atlas of senescence-associated secretomes for aging biomarker development. PLoS Biol. 18, e3000599. [PubMed: 31945054]

Bennett-Guerrero E, Swaminathan M, Grigore AM, Roach GW, Aberle LG, Johnston JM, and Fink MP (2009). A phase II multicenter double-blind placebo-controlled study of ethyl pyruvate in high-risk patients undergoing cardiac surgery with cardiopulmonary bypass. J. Cardiothorac. Vasc. Anesth 23, 324–329. [PubMed: 18835526]

Bhat R, Crowe EP, Bitto A, Moh M, Katsetos CD, Garcia FU, Johnson FB, Trojanowski JQ, Sell C, and Torres C (2012). Astrocyte senescence as a component of Alzheimer's disease. PLoS ONE 7, e45069. [PubMed: 22984612]

Bitto A, Sell C, Crowe E, Lorenzini A, Malaguti M, Hrelia S, and Torres C (2010). Stress-induced senescence in human and rodent astrocytes. Exp. Cell Res 316, 2961–2968. [PubMed: 20620137]

Boisvert MM, Erikson GA, Shokhirev MN, and Allen NJ (2018). The Aging Astrocyte Transcriptome from Multiple Regions of the Mouse Brain. Cell Rep. 22, 269–285. [PubMed: 29298427]

Bussian TJ, Aziz A, Meyer CF, Swenson BL, van Deursen JM, and Baker DJ (2018). Clearance of senescent glial cells prevents tau-dependent pathology and cognitive decline. Nature 562, 578–582. [PubMed: 30232451]

Calogero S, Grassi F, Aguzzi A, Voigtländer T, Ferrier P, Ferrari S, and Bianchi ME (1999). The lack of chromosomal protein Hmg1 does not disrupt cell growth but causes lethal hypoglycaemia in newborn mice. Nat. Genet 22, 276–280. [PubMed: 10391216]

Chen H, Guan B, Wang B, Pu H, Bai X, Chen X, Liu J, Li C, Qiu J, Yang D, et al. (2019). Glycyrrhizin Prevents Hemorrhagic Transformation and Improves Neurological Outcome in Ischemic Stroke

Author Manuscript Author Manuscript Author Manuscript Author Manuscript

with Delayed Thrombolysis Through Targeting Peroxynitrite-Mediated HMGB1 Signaling. Transl. Stroke Res 11, 967–982. [PubMed: 31872339]

Chin SS, and Goldman JE (1996). Glial inclusions in CNS degenerative diseases. J. Neuropathol. Exp. Neurol 55, 499–508. [PubMed: 8627339]

Chinta SJ, Woods G, Demaria M, Rane A, Zou Y, McQuade A, Rajagopalan S, Limbad C, Madden DT, Campisi J, and Andersen JK (2018). Cellular Senescence Is Induced by the Environmental Neurotoxin Paraquat and Contributes to Neuropathology Linked to Parkinson's Disease. Cell Rep. 22, 930–940. [PubMed: 29386135]

Chun H, Im H, Kang YJ, Kim Y, Shin JH, Won W, Lim J, Ju Y, Park YM, Kim S, et al. (2020). Severe reactive astrocytes precipitate pathological hallmarks of Alzheimer's disease via $H_2O_2^-$ production. Nat. Neurosci 23, 1555–1566. [PubMed: 33199896]

Clarke LE, Liddelow SA, Chakraborty C, Münch AE, Heiman M, and Barres BA (2018). Normal aging induces A1-like astrocyte reactivity. Proc. Natl. Acad. Sci. USA 115, E1896–E1905. [PubMed: 29437957]

Cohen J, and Torres C (2019). Astrocyte senescence: Evidence and significance. Aging Cell 18, e12937. [PubMed: 30815970]

Davalos AR, Kawahara M, Malhotra GK, Schaum N, Huang J, Ved U, Beausejour CM, Coppe JP, Rodier F, and Campisi J (2013). p53-dependent release of Alarmin HMGB1 is a central mediator of senescent phenotypes. J. Cell Biol 201, 613–629. [PubMed: 23649808]

Doody RS, Raman R, Farlow M, Iwatsubo T, Vellas B, Joffe S, Kieburtz K, He F, Sun X, Thomas RG, et al. (2013). A phase 3 trial of semagacestat for treatment of Alzheimer's disease. N. Engl. J. Med 369, 341–350. [PubMed: 23883379]

Doody RS, Farlow M, and Aisen PS; Alzheimer's Disease Cooperative Study Data Analysis and Publication Committee (2014). Phase 3 trials of solanezumab and bapineuzumab for Alzheimer's disease. N. Engl. J. Med 370, 1460.

Fakhoury M (2018). Microglia and Astrocytes in Alzheimer's Disease: Implications for Therapy. Curr. Neuropharmacol. 16, 508–518. [PubMed: 28730967]

Farmer KM, Ghag G, Puangmalai N, Montalbano M, Bhatt N, and Kayed R (2020). P53 aggregation, interactions with tau, and impaired DNA damage response in Alzheimer's disease. Acta Neuropathol. Commun 8, 132. [PubMed: 32778161]

Fink MP (2007). Ethyl pyruvate: a novel anti-inflammatory agent. J. Intern. Med 261, 349–362. [PubMed: 17391109]

Fonken LK, Frank MG, Kitt MM, D'Angelo HM, Norden DM, Weber MD, Barrientos RM, Godbout JP, Watkins LR, and Maier SF (2016). The Alarmin HMGB1 Mediates Age-Induced Neuroinflammatory Priming. J. Neurosci 36, 7946–7956. [PubMed: 27466339]

Forman MS, Lal D, Zhang B, Dabir DV, Swanson E, Lee VM, and Trojanowski JQ (2005). Transgenic mouse model of tau pathology in astrocytes leading to nervous system degeneration. J. Neurosci 25, 3539–3550. [PubMed: 15814784]

Freund A, Patil CK, and Campisi J (2011). p38MAPK is a novel DNA damage response-independent regulator of the senescence-associated secretory phenotype. EMBO J. 30, 1536–1548. [PubMed: 21399611]

Fujita K, Motoki K, Tagawa K, Chen X, Hama H, Nakajima K, Homma H, Tamura T, Watanabe H, Katsuno M, et al. (2016). HMGB1, a pathogenic molecule that induces neurite degeneration via TLR4-MARCKS, is a potential therapeutic target for Alzheimer's disease. Sci. Rep 6, 31895. [PubMed: 27557632]

Funayama A, Shishido T, Netsu S, Narumi T, Kadowaki S, Takahashi H, Miyamoto T, Watanabe T, Woo CH, Abe J, et al. (2013). Cardiac nuclear high mobility group box 1 prevents the development of cardiac hypertrophy and heart failure. Cardiovasc. Res 99, 657–664. [PubMed: 23708738]

Gerson J, Castillo-Carranza DL, Sengupta U, Bodani R, Prough DS, DeWitt DS, Hawkins BE, and Kayed R (2016). Tau Oligomers Derived from Traumatic Brain Injury Cause Cognitive Impairment and Accelerate Onset of Pathology in Htau Mice. J. Neurotrauma 33, 2034–2043. [PubMed: 26729399]

Author Manuscript Author Manuscript Author Manuscript Author Manuscript

Gerson JE, Sengupta U, and Kayed R (2017). Tau Oligomers as Pathogenic Seeds: Preparation and Propagation In Vitro and In Vivo. Methods Mol. Biol 1523, 141–157. [PubMed: 27975249]

Ghag G, Bhatt N, Cantu DV, Guerrero-Munoz MJ, Ellsworth A, Sengupta U, and Kayed R (2018). Soluble tau aggregates, not large fibrils, are the toxic species that display seeding and cross-seeding behavior. Protein Sci 27, 1901–1909. [PubMed: 30125425]

Golde TE, Schneider LS, and Koo EH (2011). Anti-aβ therapeutics in Alzheimer's disease: the need for a paradigm shift. Neuron 69, 203–213. [PubMed: 21262461]

Gomez-Tortosa E, Baradaran-Heravi Y, Gonzalez Alvarez V, Sainz MJ, Prieto-Jurczynska C, Guerrero-Lopez R, Aguero Rabes P, Van Broeckhoven C, van der Zee J, Rabano Gutierrez A, et al. (2019). Presence of tau astrogliopathy in frontotemporal dementia caused by a novel Grn nonsense (Trp2*) mutation. Neurobiol. Aging 76, 214.e211–214.e215.

González-Reyes RE, Nava-Mesa MO, Vargas-Sánchez K, Ariza-Salamanca D, and Mora-Murñoz L (2017). Involvement of Astrocytes in Alzheimer's Disease from a Neuroinflammatory and Oxidative Stress Perspective. Front. Mol. Neurosci 10, 427. [PubMed: 29311817]

Guzman-Martinez L, Maccioni RB, Andrade V, Navarrete LP, Pastor MG, and Ramos-Escobar N (2019). Neuroinflammation as a Common Feature of Neurodegenerative Disorders. Front. Pharmacol 10, 1008. [PubMed: 31572186]

Han X, Zhang T, Liu H, Mi Y, and Gou X (2020). Astrocyte Senescence and Alzheimer's Disease: A Review. Front. Aging Neurosci 12, 148. [PubMed: 32581763]

Heithoff BP, George KK, Phares AN, Zuidhoek IA, Munoz-Ballester C, and Robel S (2021). Astrocytes are necessary for blood-brain barrier maintenance in the adult mouse brain. Glia 69, 436–472. [PubMed: 32955153]

Hou S, Zhang T, Li Y, Guo F, and Jin X (2017). Glycyrrhizic Acid Prevents Diabetic Nephropathy by Activating AMPK/SIRT1/PGC-1α Signaling in db/db Mice. J. Diabetes Res 2017, 2865912. [PubMed: 29238727]

Hyman BT (2014). Tau propagation, different tau phenotypes, and prion-like properties of tau. Neuron 82, 1189–1190. [PubMed: 24945760]

Iram T, Trudler D, Kain D, Kanner S, Galron R, Vassar R, Barzilai A, Blinder P, Fishelson Z, and Frenkel D (2016). Astrocytes from old Alzheimer's disease mice are impaired in Aβ uptake and in neuroprotection. Neurobiol. Dis 96, 84–94. [PubMed: 27544484]

Ising C, Venegas C, Zhang S, Scheiblich H, Schmidt SV, Vieira-Saecker A, Schwartz S, Albasset S, McManus RM, Tejera D, et al. (2019). NLRP3 inflammasome activation drives tau pathology. Nature 575, 669–673. [PubMed: 31748742]

Iwasa H, Han J, and Ishikawa F (2003). Mitogen-activated protein kinase p38 defines the common senescence-signalling pathway. Genes Cells 8, 131–144. [PubMed: 12581156]

Jeon OH, Kim C, Laberge RM, Demaria M, Rathod S, Vasserot AP, Chung JW, Kim DH, Poon Y, David N, et al. (2017). Local clearance of senescent cells attenuates the development of post-traumatic osteoarthritis and creates a pro-regenerative environment. Nat. Med 23, 775–781. [PubMed: 28436958]

Kim DE, and Davalos AR (2019). Alarmin Detection in Senescent Cells. Methods Mol. Biol 1896, 71–81. [PubMed: 30474841]

Kim YM, Park EJ, Kim JH, Park SW, Kim HJ, and Chang KC (2016). Ethyl pyruvate inhibits the acetylation and release of HMGB1 via effects on SIRT1/STAT signaling in LPS-activated RAW264.7 cells and peritoneal macrophages. Int. Immunopharmacol. 41, 98–105. [PubMed: 27865166]

Kovacs GG (2020). Astroglia and Tau: New Perspectives. Front. Aging Neurosci. 12, 96. [PubMed: 32327993]

Kovacs GG, Ferrer I, Grinberg LT, Alafuzoff I, Attems J, Budka H, Cairns NJ, Crary JF, Duyckaerts C, Ghetti B, et al. (2016). Aging-related tau astrogliopathy (ARTAG): harmonized evaluation strategy. Acta Neuropathol. 131, 87–102. [PubMed: 26659578]

Kovacs GG, Lee VM, and Trojanowski JQ (2017a). Protein astrogliopathies in human neurodegenerative diseases and aging. Brain Pathol. 27, 675–690. [PubMed: 28805003]

Author Manuscript Author Manuscript Author Manuscript Author Manuscript

Kovacs GG, Xie SX, Lee EB, Robinson JL, Caswell C, Irwin DJ, Toledo JB, Johnson VE, Smith DH, Alafuzoff I, et al. (2017b). Multisite Assessment of Aging-Related Tau Astrogliopathy (ARTAG). J. Neuropathol. Exp. Neurol 76, 605–619. [PubMed: 28591867]

Kwon YJ, Son DH, Chung TH, and Lee YJ (2020).A Review of the Pharmacological Efficacy and Safety of Licorice Root from Corroborative Clinical Trial Findings. J. Med. Food 23, 12–20. [PubMed: 31874059]

Lasagna-Reeves CA, Castillo-Carranza DL, Guerrero-Muoz MJ, Jackson GR, and Kayed R (2010). Preparation and characterization of neurotoxic tau oligomers. Biochemistry 49, 10039–10041. [PubMed: 21047142]

Lasagna-Reeves CA, Castillo-Carranza DL, Sengupta U, Sarmiento J, Troncoso J, Jackson GR, and Kayed R (2012). Identification of oligomers at early stages of tau aggregation in Alzheimer's disease. FASEB J. 26, 1946–1959. [PubMed: 22253473]

Lee SH, Lee JH, Lee HY, and Min KJ (2019). Sirtuin signaling in cellular senescence and aging. BMB Rep. 52, 24–34. [PubMed: 30526767]

Limbad C, Oron TR, Alimirah F, Davalos AR, Tracy TE, Gan L, Desprez PY, and Campisi J (2020). Astrocyte senescence promotes glutamate toxicity in cortical neurons. PLoS ONE 15, e0227887. [PubMed: 31945125]

Lotze MT, and Tracey KJ (2005). High-mobility group box 1 protein (HMGB1): nuclear weapon in the immune arsenal. Nat. Rev. Immunol 5, 331–342. [PubMed: 15803152]

Ly PT, Cai F, and Song W (2011). Detection of neuritic plaques in Alzheimer's disease mouse model. J. Vis. Exp 53, 2831.

Lye JJ, Latorre E, Lee BP, Bandinelli S, Holley JE, Gutowski NJ, Ferrucci L, and Harries LW (2019). Astrocyte senescence may drive alterations in GFAPα, CDKN2A $p14^{ARF}$, and TAU3 transcript expression and contribute to cognitive decline. Geroscience 41, 561–573. [PubMed: 31654269]

Maeda S, Sahara N, Saito Y, Murayama S, Ikai A, and Takashima A (2006). Increased levels of granular tau oligomers: an early sign of brain aging and Alzheimer's disease. Neurosci. Res 54, 197–201. [PubMed: 16406150]

McCarthy KD, and deVellis J (1980). Preparation of separate astroglial and oligodendroglial cell cultures from rat cerebral tissue. J. Cell Biol 85, 890–902. [PubMed: 6248568]

Menon R, Behnia F, Polettini J, Saade GR, Campisi J, and Velarde M (2016). Placental membrane aging and HMGB1 signaling associated with human parturition. Aging (Albany NY) 8, 216–230. [PubMed: 26851389]

Ming GL, and Song H (2011). Adult neurogenesis in the mammalian brain: significant answers and significant questions. Neuron 70, 687–702. [PubMed: 21609825]

Mollica L, De Marchis F, Spitaleri A, Dallacosta C, Pennacchini D, Zamai M, Agresti A, Trisciuoglio L, Musco G, and Bianchi ME (2007). Glycyrrhizin binds to high-mobility group box 1 protein and inhibits its cytokine activities. Chem. Biol 14, 431–441. [PubMed: 17462578]

Montalbano M, McAllen S, Puangmalai N, Sengupta U, Bhatt N, Johnson OD, Kharas MG, and Kayed R (2020). RNA-binding proteins Musashi and tau soluble aggregates initiate nuclear dysfunction. Nat. Commun 11, 4305. [PubMed: 32855391]

Morsch R, Simon W, and Coleman PD (1999). Neurons may live for decades with neurofibrillary tangles. J. Neuropathol. Exp. Neurol 58, 188–197. [PubMed: 10029101]

Musi N, Valentine JM, Sickora KR, Baeuerle E, Thompson CS, Shen Q, and Orr ME (2018). Tau protein aggregation is associated with cellular senescence in the brain. Aging Cell 17, e12840. [PubMed: 30126037]

Nicaise AM, Wagstaff LJ, Willis CM, Paisie C, Chandok H, Robson P, Fossati V, Williams A, and Crocker SJ (2019). Cellular senescence in progenitor cells contributes to diminished remyelination potential in progressive multiple sclerosis. Proc. Natl. Acad. Sci. USA 116, 9030–9039. [PubMed: 30910981]

Nilson AN, English KC, Gerson JE, Barton Whittle T, Nicolas Crain C, Xue J, Sengupta U, Castillo-Carranza DL, Zhang W, Gupta P, and Kayed R (2017). Tau Oligomers Associate with Inflammation in the Brain and Retina of Tauopathy Mice and in Neurodegenerative Diseases. J. Alzheimers Dis 55, 1083–1099. [PubMed: 27716675]

Author Manuscript Author Manuscript Author Manuscript Author Manuscript

Nolan A, De Paula Franca Resende, E., Petersen C, Neylan K, Spina S, Huang E, Seeley W, Miller Z, and Grinberg LT. (2019). Astrocytic Tau Deposition Is Frequent in Typical and Atypical Alzheimer Disease Presentations. J. Neuropathol. Exp. Neurol 78, 1112–1123. [PubMed: 31626288]

Oeckl P, Halbgebauer S, Anderl-Straub S, Steinacker P, Huss AM, Neugebauer H, von Arnim CAF, Diehl-Schmid J, Grimmer T, Kornhuber J, et al. (2019). Glial Fibrillary Acidic Protein in Serum is Increased in Alzheimer's Disease and Correlates with Cognitive Impairment. J. Alzheimers Dis 67, 481–488. [PubMed: 30594925]

Ogrodnik M, Salmonowicz H, Jurk D, and Passos JF (2019). Expansion and Cell-Cycle Arrest: Common Denominators of Cellular Senescence.Trends Biochem. Sci 44, 996–1008. [PubMed: 31345557]

Paudel YN, Shaikh MF, Chakraborti A, Kumari Y, Aledo-Serrano A, Aleksovska K, Alvim MKM, and Othman I (2018). HMGB1: A Common Biomarker and Potential Target for TBI, Neuroinflammation, Epilepsy, and Cognitive Dysfunction. Front. Neurosci 12, 628. [PubMed: 30271319]

Paudel YN, Angelopoulou E, Piperi C, Othman I, Aamir K, and Shaikh MF (2020). Impact of HMGB1, RAGE, and TLR4 in Alzheimer's Disease (AD): From Risk Factors to Therapeutic Targeting. Cells 9, 383.

Perez-Nievas BG, and Serrano-Pozo A (2018). Deciphering the Astrocyte Reaction in Alzheimer's Disease. Front. Aging Neurosci 10, 114. [PubMed: 29922147]

Pernègre C, Duquette A, and Leclerc N (2019). Tau Secretion: Good and Bad for Neurons. Front. Neurosci 13, 649. [PubMed: 31293374]

Piacentini R, Li Puma DD, Mainardi M, Lazzarino G, Tavazzi B, Arancio O, and Grassi C (2017). Reduced gliotransmitter release from astrocytes mediates tau-induced synaptic dysfunction in cultured hippocampal neurons. Glia 65, 1302–1316. [PubMed: 28519902]

Polydoro M, Acker CM, Duff K, Castillo PE, and Davies P (2009). Age-dependent impairment of cognitive and synaptic function in the htau mouse model of tau pathology. J. Neurosci 29, 10741–10749. [PubMed: 19710325]

Puangmalai N, Bhatt N, Montalbano M, Sengupta U, Gaikwad S, Ventura F, McAllen S, Ellsworth A, Garcia S, and Kayed R (2020). Internalization mechanisms of brain-derived tau oligomers from patients with Alzheimer's disease, progressive supranuclear palsy and dementia with Lewy bodies. Cell Death Dis. 11, 314. [PubMed: 32366836]

Rauch JN, Luna G, Guzman E, Audouard M, Challis C, Sibih YE, Leshuk C, Hernandez I, Wegmann S, Hyman BT, et al. (2020). LRP1 is a master regulator of tau uptake and spread. Nature 580, 381–385. [PubMed: 32296178]

Reid MJ, Beltran-Lobo P, Johnson L, Perez-Nievas BG, and Noble W (2020). Astrocytes in Tauopathies. Front. Neurol 11, 572850. [PubMed: 33071951]

Richetin K, Steullet P, Pachoud M, Perbet R, Parietti E, Maheswaran M, Eddarkaoui S, Bégard S, Pythoud C, Rey M, et al. (2020). Tau accumulation in astrocytes of the dentate gyrus induces neuronal dysfunction and memory deficits in Alzheimer's disease. Nat. Neurosci 23, 1567–1579. [PubMed: 33169029]

Salminen A, Ojala J, Kaarniranta K, Haapasalo A, Hiltunen M, and Soininen H (2011). Astrocytes in the aging brain express characteristics of senescence-associated secretory phenotype. Eur. J. Neurosci 34, 3–11. [PubMed: 21649759]

Salminen A, Kauppinen A, and Kaarniranta K (2012). Emerging role of NF-κB signaling in the induction of senescence-associated secretory phenotype (SASP). Cell. Signal 24, 835–845. [PubMed: 22182507]

Satoh A, Brace CS, Rensing N, Cliften P, Wozniak DF, Herzog ED, Yamada KA, and Imai S (2013). Sirt1 extends life span and delays aging in mice through the regulation of Nk2 homeobox 1 in the DMH and LH. Cell Metab. 18, 416–430. [PubMed: 24011076]

Schildge S, Bohrer C, Beck K, and Schachtrup C (2013). Isolation and culture of mouse cortical astrocytes. J. Vis. Exp 71, 50079.

Sengupta U, Portelius E, Hansson O, Farmer K, Castillo-Carranza D, Woltjer R, Zetterberg H, Galasko D, Blennow K, and Kayed R (2017). Tau oligomers in cerebrospinal fluid in Alzheimer's disease. Ann. Clin. Transl. Neurol 4, 226–235. [PubMed: 28382304]

Author Manuscript Author Manuscript Author Manuscript Author Manuscript

Shafiei SS, Guerrero-Muñoz MJ, and Castillo-Carranza DL (2017). Tau Oligomers: Cytotoxicity, Propagation, and Mitochondrial Damage. Front. Aging Neurosci 9, 83. [PubMed: 28420982]

Shen H, Hu X, Liu C, Wang S, Zhang W, Gao H, Stetler RA, Gao Y, and Chen J (2010). Ethyl pyruvate protects against hypoxic-ischemic brain injury via anti-cell death and anti-inflammatory mechanisms. Neurobiol. Dis 37, 711–722. [PubMed: 20026271]

Sun Y, Chen H, Dai J, Wan Z, Xiong P, Xu Y, Han Z, Chai W, Gong F, and Zheng F (2018). Glycyrrhizin Protects Mice Against Experimental Autoimmune Encephalomyelitis by Inhibiting High-Mobility Group Box 1 (HMGB1) Expression and Neuronal HMGB1 Release. Front. Immunol 9, 1518. [PubMed: 30013568]

Tang Q, Cao Y, Xiong W, Ke X, Zhang J, Xia Y, and Liu D (2020). Glycyrrhizic acid exerts protective effects against hypoxia/reoxygenation-induced human coronary artery endothelial cell damage by regulating mitochondria. Exp. Ther. Med 20, 335–342. [PubMed: 32509013]

Ulloa L, Ochani M, Yang H, Tanovic M, Halperin D, Yang R, Czura CJ, Fink MP, and Tracey KJ (2002). Ethyl pyruvate prevents lethality in mice with established lethal sepsis and systemic inflammation. Proc. Natl. Acad. Sci. USA 99, 12351–12356. [PubMed: 12209006]

Vasile F, Dossi E, and Rouach N (2017). Human astrocytes: structure and functions in the healthy brain. Brain Struct. Funct 222, 2017–2029. [PubMed: 28280934]

Victorelli S, Lagnado A, Halim J, Moore W, Talbot D, Barrett K, Chapman J, Birch J, Ogrodnik M, Meves A, et al. (2019). Senescent human melanocytes drive skin ageing via paracrine telomere dysfunction. EMBO J. 38, e101982. [PubMed: 31633821]

Wang H, Li W, Goldstein R, Tracey KJ, and Sama AE (2007). HMGB1 as a potential therapeutic target. Novartis Found. Symp 280, 73–85, discussion 85–91, 160–164.

Xu M, Pirtskhalava T, Farr JN, Weigand BM, Palmer AK, Weivoda MM, Inman CL, Ogrodnik MB, Hachfeld CM, Fraser DG, et al. (2018). Senolytics improve physical function and increase lifespan in old age. Nat. Med 24, 1246–1256. [PubMed: 29988130]

Zandarashvili L, Sahu D, Lee K, Lee YS, Singh P, Rajarathnam K, and Iwahara J (2013). Real-time kinetics of high-mobility group box 1 (HMGB1) oxidation in extracellular fluids studied by in situ protein NMR spectroscopy. J. Biol. Chem 288, 11621–11627. [PubMed: 23447529]

Zhang Y, Sloan SA, Clarke LE, Caneda C, Plaza CA, Blumenthal PD, Vogel H, Steinberg GK, Edwards MS, Li G, et al. (2016). Purification and Characterization of Progenitor and Mature Human Astrocytes Reveals Transcriptional and Functional Differences with Mouse. Neuron 89, 37–53. [PubMed: 26687838]

Zhang P, Kishimoto Y, Grammatikakis I, Gottimukkala K, Cutler RG, Zhang S, Abdelmohsen K, Bohr VA, Misra Sen J, Gorospe M, and Mattson MP (2019a). Senolytic therapy alleviates Aβ-associated oligodendrocyte progenitor cell senescence and cognitive deficits in an Alzheimer's disease model. Nat. Neurosci 22, 719–728. [PubMed: 30936558]

Zhang T, Guan XW, Gribben JG, Liu FT, and Jia L (2019b). Blockade of HMGB1 signaling pathway by ethyl pyruvate inhibits tumor growth in diffuse large B-cell lymphoma. Cell Death Dis. 10, 330. [PubMed: 30988279]

Zhao F, Fang Y, Deng S, Li X, Zhou Y, Gong Y, Zhu H, and Wang W (2017). Glycyrrhizin Protects Rats from Sepsis by Blocking HMGB1 Signaling. BioMed Res. Int. 2017, 9719647. [PubMed: 28484719]

Zhao J, Wu H, and Tang XQ (2021). Tau internalization: A complex step in tau propagation. Ageing Res. Rev 67, 101272. [PubMed: 33571704]

Author Manuscript Author Manuscript Author Manuscript Author Manuscript

Highlights

- Postmortem AD and FTD brain tissues exhibit TauO-associated senescent astrocytes
- Direct exposure of TauO triggers cellular senescence in cultured astrocytes
- HMGB1 release is a crucial event during TauO-induced cellular senescence
- HMGB1 released by senescent cells may contribute to the progression of tauopathies

Author Manuscript
Author Manuscript
Author Manuscript
Author Manuscript

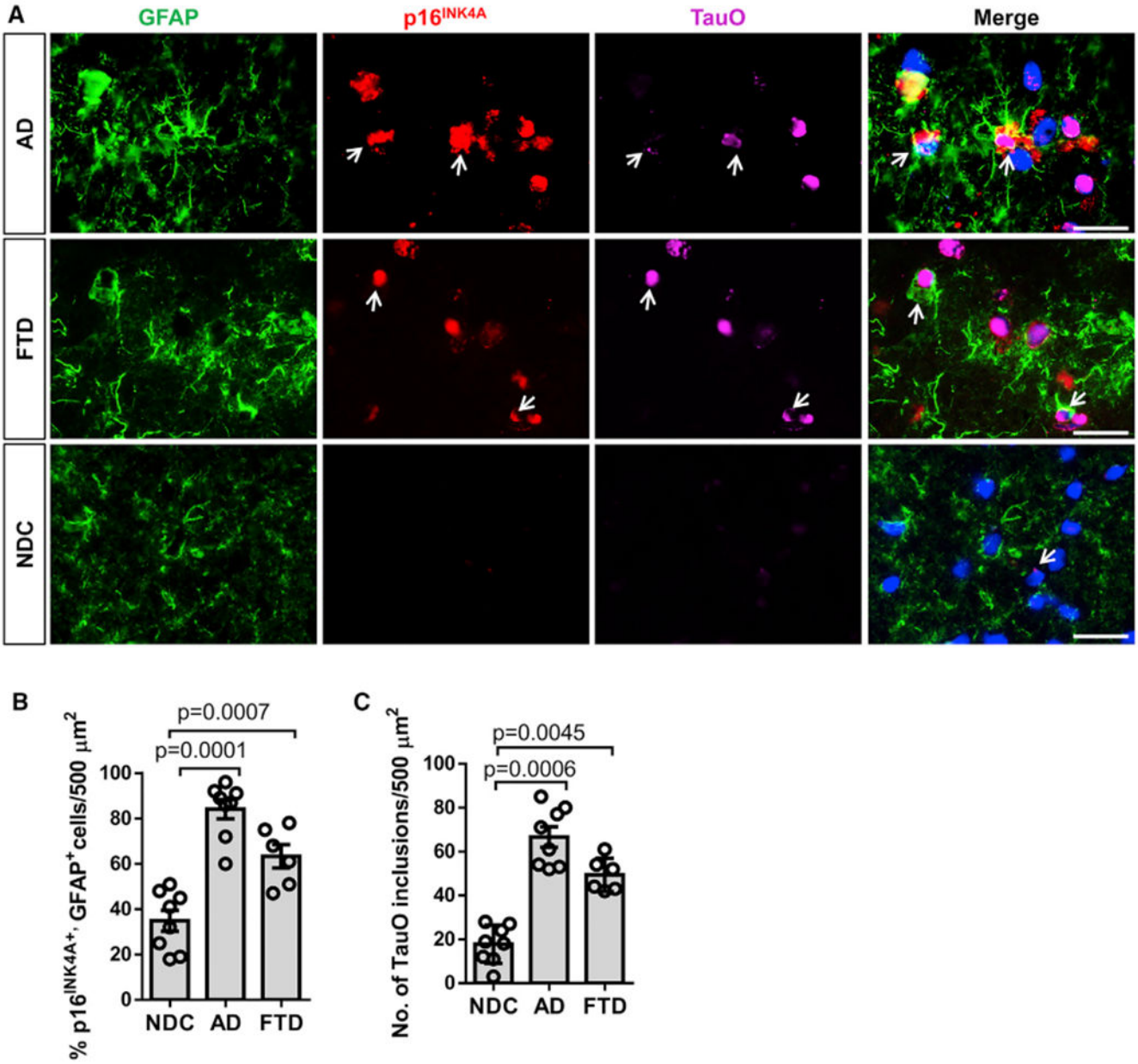

Figure 1. Astrocytes exhibiting a senescence-like phenotype are associated with TauO in the brain of patients with AD and FTD

(A) Representative immunostaining showing GFAP (green), $p16^{INK4A}$ (red), and TauO (magenta) immunoreactivities and DAPI (blue nuclei) in sections of the frontal cortex from patients with AD and FTD and NDC subjects. In AD and FTD brains, triple immunostaining displays colocalization of $p16^{INK4A}$ and TauO immunoreactivities in GFAP-positive astrocytes. Only a small percentage of cells display $p16^{INK4A}$ and TauO in the NDC brain. Arrows indicate TauO-associated cells exhibiting $p16^{INK4A}$ and GFAP immunoreactivities in AD and FTD.

(B and C) Percentage of $p16^{INK4A}$-positive and GFAP-positive cells, and (C) average numbers of TauO inclusions per 500 μm^2 (mean ± SEM; AD n = 8 cases, FTD n = 6 cases,

and NDC n = 8 cases; minimum 6–8 images were analyzed from each section). One-way ANOVA followed by Tukey's post hoc test was used to determine the statistical differences among the groups. Scale bars, 20 μm.

Author Manuscript Author Manuscript Author Manuscript Author Manuscript

Author Manuscript Author Manuscript Author Manuscript Author Manuscript

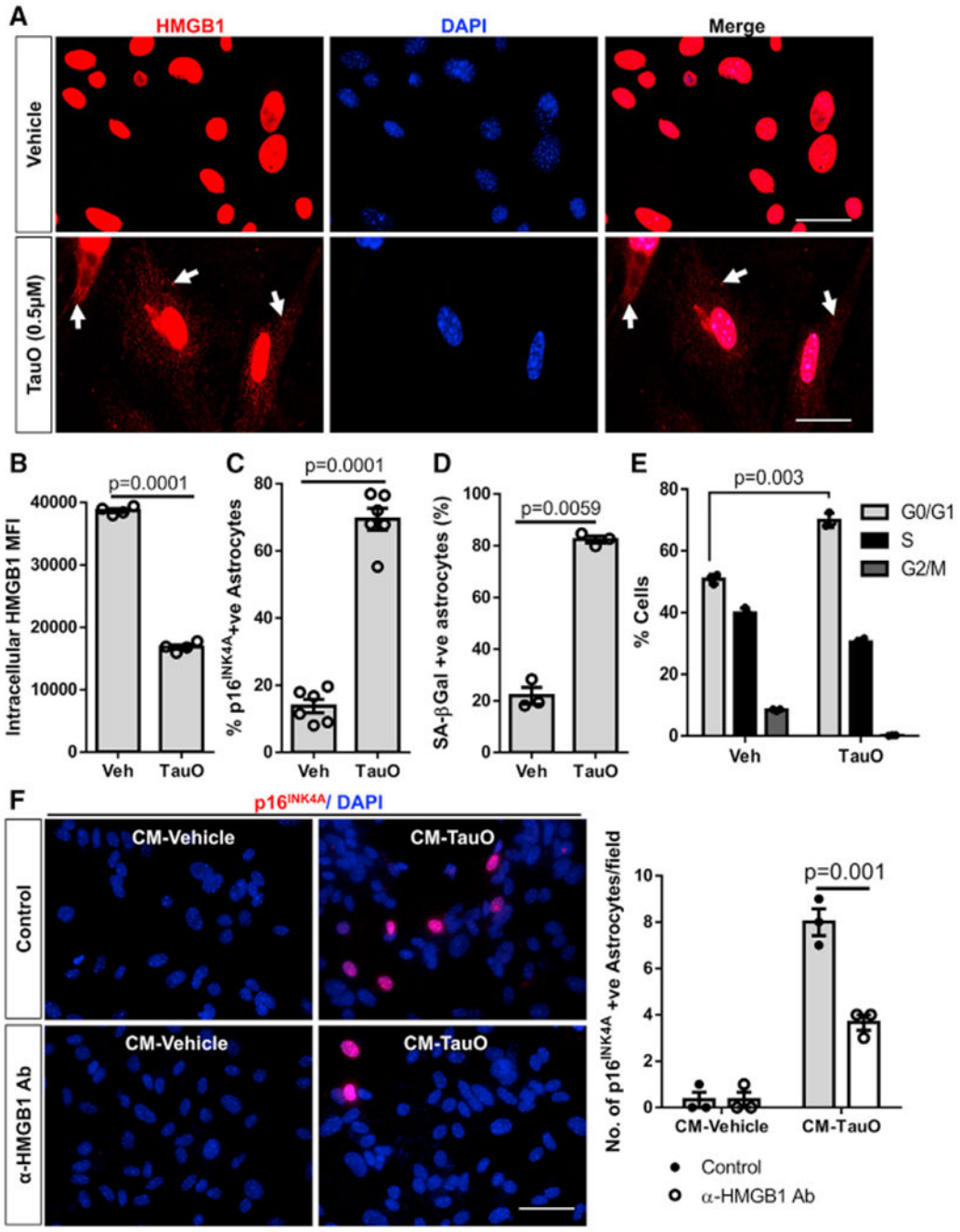

Figure 2. Nucleo-cytoplasmic translocation and active release of HMGB1 is a hallmark of TauO-induced senescence phenotype in primary astrocytes

(A–F) Upon stimulation with TauO or vehicle for 11 days, astrocytes were examined for HMGB1 translocation and release by immunostaining and flow cytometry analysis, respectively. Arrows point to TauO-induced translocation of HMGB1, a signature of cellular senescence. Scale bars, 50 μm. TauO exposure significantly increased $p16^{INK4A}$-positive astrocytes (C), the percentage of SA-β-gal-positive astrocytes (D), and cell-cycle arrest (E) $p16^{INK4A}$ staining (F) after 4 days of treatment with or without conditional media (CM) from senescent astrocytes in the presence or absence of α-HMGB1 antibody (4 μg/mL).

Author Manuscript Author Manuscript Author Manuscript Author Manuscript

Representative images showing the relative decrease in number of $p16^{INK4A}$-positive astrocytes after α-HMGB1 antibody treatment. Scale bar, 50 μm. Data are representative of at least three independent experiments (mean ± SEM). Statistical analyses were measured by unpaired, two-tailed Student's t test.

Author Manuscript
Author Manuscript
Author Manuscript
Author Manuscript

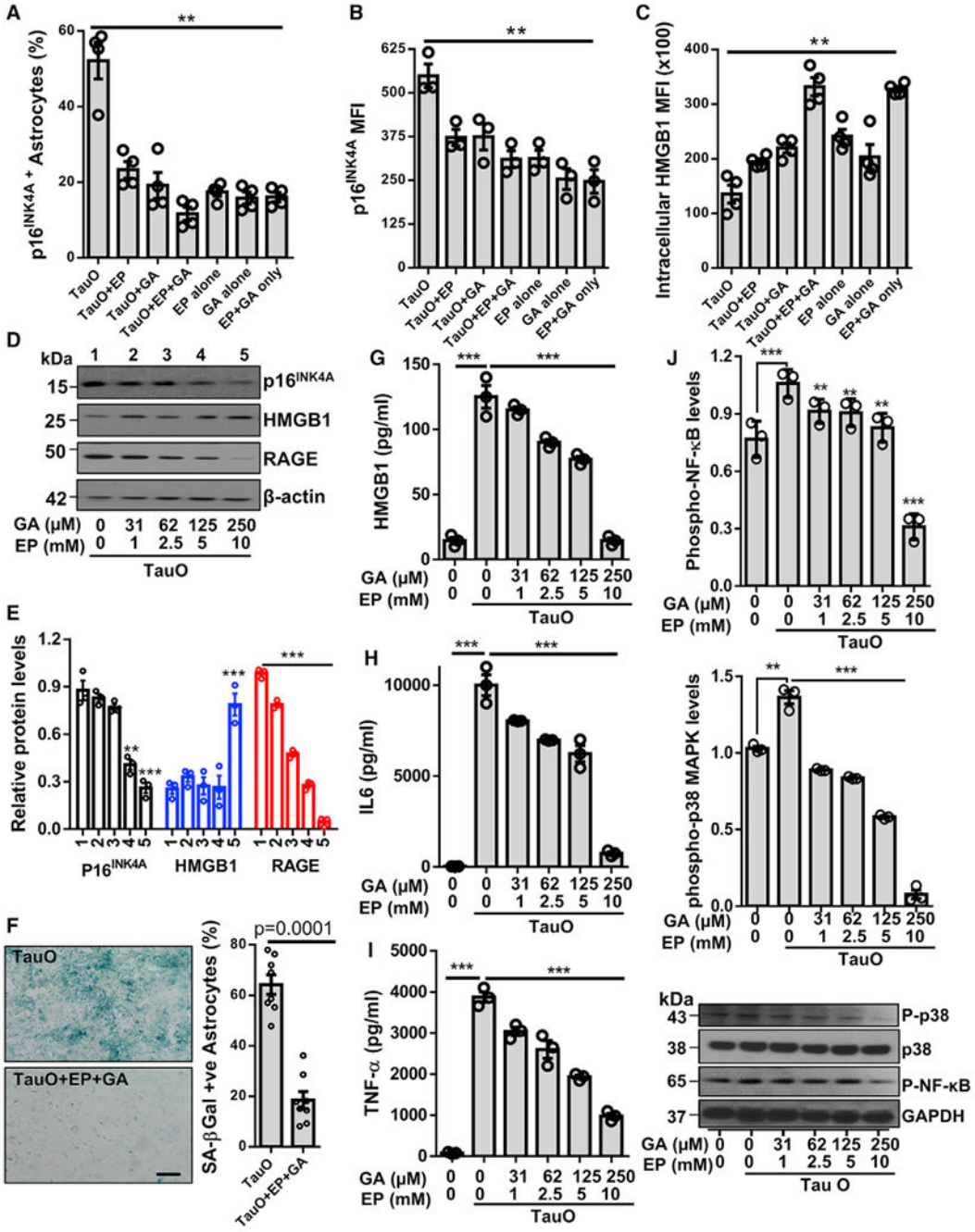

Figure 3. Inhibition of HMGB1 signaling effectively prevents TauO-induced senescence-like phenotype in cultured astrocytes

Primary astrocytes were cultured in poly-L-lysine (PLL)-coated plates for 48 h and then pretreated with or without HMGB1 release inhibitors EP (10 mM) and/or GA (250 μM) for 30 min followed by treatment with TauO (0.5 μM) for 11 days.

(A–C) HMGB1 release inhibition prevents TauO-induced astrocyte senescence, as shown by the decreased percentage of $p16^{INK4A}$-positive cells and $p16^{INK4A}$ mean fluorescence intensity (MFI) and increased MFI of intracellular HMGB1 by flow cytometry.

Representative graphs are shown from a minimum of three to four independent experiments

Author Manuscript Author Manuscript Author Manuscript Author Manuscript

(mean ± SEM). Statistical significance was determined by using one-way ANOVA followed by Tukey's post hoc test (**p < 0.05; ***p < 0.0001).

(D and E) Effect of EP+GA on relative protein levels of $p16^{INK4A}$, HMGB1, and RAGE was measured by immunoblotting followed by densitometry quantification; β-actin was used as a loading control. The densitometry bar graph is numbered as in blots. Data are shown as mean ± SEM. Statistical significance was determined by using one-way ANOVA followed by Tukey's post hoc test (**p < 0.05; ***p < 0.0001).

(F) Effect of EP+GA on TauO-induced astrocyte senescence was measured by SA-β-gal staining. Pretreatment with EP (10 mM) + GA (250 μM) attenuated TauO-induced astrocytes senescence-like phenotype as shown by decreased SA-β-gal activity. Scale bar, 50 μm. Data are shown as mean ± SEM from four independent experiments in duplicates. Statistical significance was determined using unpaired, two-tailed Student's t test.

(G–I) Conditioned media from the astrocytes culture were used to measure secreted levels of HMGB1, (H) IL-6, and (I) TNF-α using ELISA showing HMGB1 inhibitors effectively inhibit TauO-induced SASP activity. Data are mean ± SEM from at least three independent experiments. Statistical analysis was performed by one-way ANOVA followed by Tukey's post hoc test.

(J) Phosphorylated protein levels of p38 and NF-κB assayed by immunoblotting, followed by densitometry quantification; GAPDH was used as a loading control. Data are shown as mean ± SEM (*p < 0.05; **p < 0.001; ***p < 0.0001).

Author Manuscript Author Manuscript Author Manuscript Author Manuscript

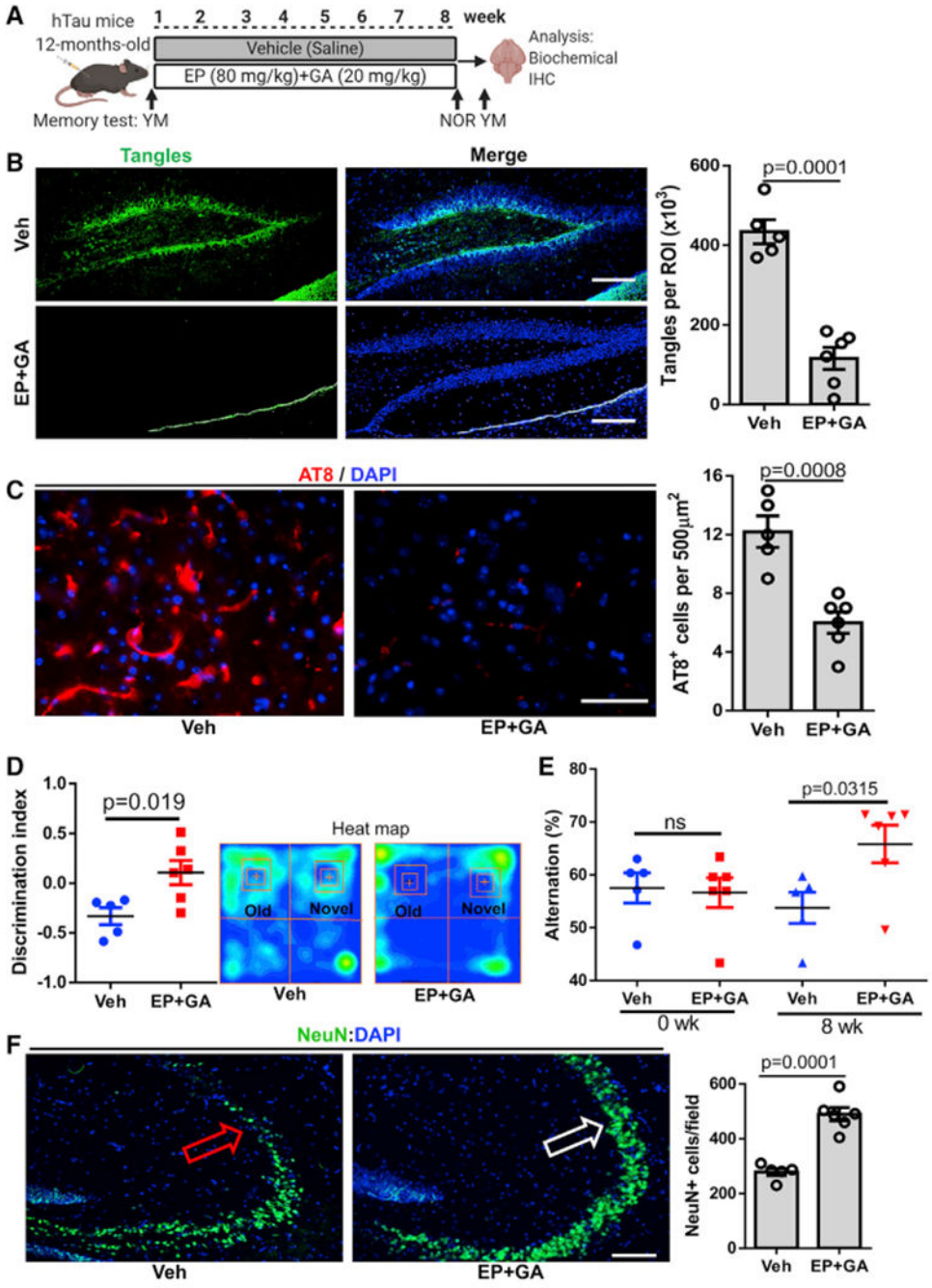

Figure 4. Treatment with HMGB1 release inhibitors ameliorates tau pathology and cognitive decline in hTau mice

(A) Experimental design for 8-week treatment with HMGB1 release inhibitors EP (80 mg/kg) + GA (20 mg/kg) or vehicle (saline) three times per week, beginning at 12 months of age in hTau mice.

(B) Images of thioflavin-S staining and quantification of NFTs (tangles per region of interest) in the hippocampus. Scale bars, 200 μm. Data are shown as the mean ± SEM.

(C) Representative immunostaining images showing hyperphosphorylated tau (AT8 immunoreactivities) in the hippocampus of hTau mice treated with either saline or EP+GA

Author Manuscript Author Manuscript Author Manuscript Author Manuscript

(scale bars, 50 μm) and quantification of AT8-positive cells per 500 μm^2. Data are the mean ± SEM; unpaired, two-tailed Student's t test was used to determine the statistical differences.

(D) Novel-object recognition task was used to measure the impact of EP+GA treatment on memory in hTau mice. Mice treated with EP+GA show significantly higher discrimination index than vehicle-treated mice; heatmap of representative mice from the vehicle and EP +GA treatment group showing the time spent on exploring old or novel objects. Statistical significance was determined using unpaired, two-tailed Student's t test.

(E) Y-maze spontaneous alternation test: percentage of spontaneous alterations were measured before and after 8 weeks of EP+GA or vehicle treatment. Data are the mean ± SEM; unpaired, two-tailed Student's t test was used to determine the statistical differences.

(F) Immunostaining showing NeuN-positive neuronal cells in the CA3 pyramidal layer of the hippocampus of hTau mice treated with either vehicle or EP+GA. Scale bar, 100 μm. Data are the mean ± SEM; unpaired, two-tailed Student's t test was used to determine the statistical differences.

Author Manuscript Author Manuscript Author Manuscript Author Manuscript

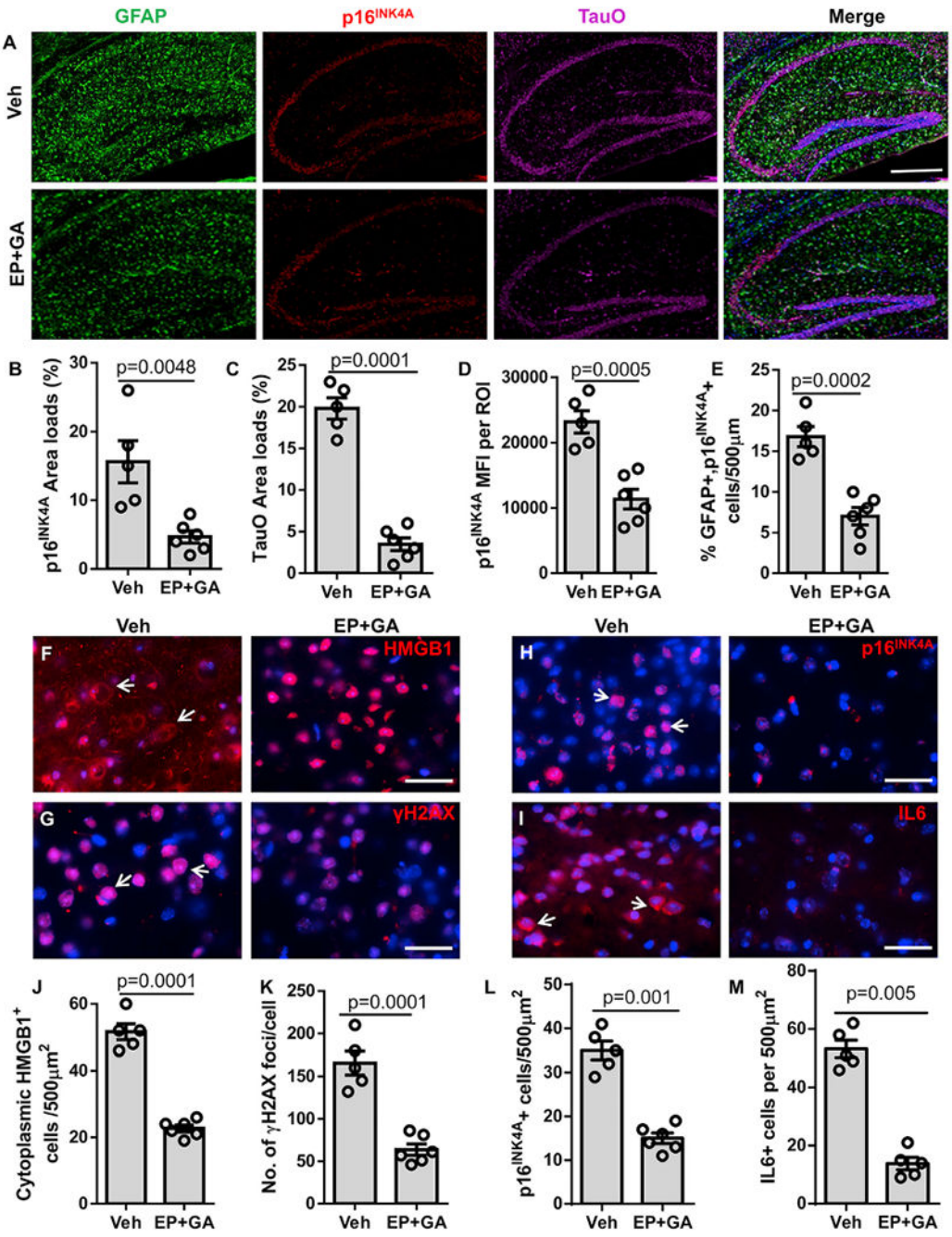

Figure 5. HMGB1 release inhibitors treatment modulates TauO-associated senescent cells in 12-month-old hTau mice

(A) Representative immunostaining images and quantification of TauO-associated senescent astrocytes in the hippocampus. Representative immunostaining showing GFAP (green), $p16^{INK4A}$ (red), and TauO (magenta) immunoreactivities and DAPI (blue nuclei) in the hippocampus of hTau mice treated with either vehicle or EP+GA. Images display colocalization of $p16^{INK4A}$ and TauO in GFAP-positive astrocytes.

(B–E) The graph showing quantitative analysis of $p16^{INK4A}$ area load (B), TauO area load (C), $p16^{INK4A}$ MFI (D), and percentage of $p16^{INK4A}$-positive and GFAP-positive cells (E) in

Author Manuscript Author Manuscript Author Manuscript Author Manuscript

the hippocampus of hTau mice treated with vehicle (n = 5 mice) and EP+GA (n = 6 mice). Data are shown as mean ± SEM; unpaired, two-tailed Student's t test was used to determine the statistical differences. Scale bars, 200 μm.

(F–M) Immunostaining quantification of cytoplasmic HMGB1-positive cells (F and J), number of γH2AX foci (G and K), $p16^{INK4A}$-positive cells (H and L), and IL-6-positive cells (I and M) in the cortex of hTau mice treated with vehicle (n = 5 mice) and EP+GA (n = 6 mice). Data are shown as mean ± SEM; unpaired, two-tailed Student's t test was used to determine the statistical differences. Scale bar, 20 μm.

Author Manuscript Author Manuscript Author Manuscript Author Manuscript

KEY RESOURCES TABLE

REAGENT or RESOURCE	SOURCE	IDENTIFIER
Antibodies		
Human-p16INK4A (D3W8G) antibody	Cell Signaling Technology	Cat#92803; RRID:AB_2750891
Mouse-p16INK4A (M-156) antibody	Santa Cruz Biotechnology	Cat# sc-1207; RRID:AB_632106
Phospho-Histone H2A.X (Ser139) (20E3), antibody	Cell Signaling Technology	Cat#9718; RRID: AB_2118009
IL-6 (D5W4V) antibody	Cell Signaling Technology	Cat# 12912; RRID:AB_2687897
Anti-HMGB1 antibody	Abcam	Cat#ab18256; RRID:AB_444360
Anti-RAGE antibody	Abcam	Cat#ab37647; RRID:AB_777613
Monoclonal Anti-β-Actin–Peroxidase antibody	Sigma	Cat#A3854; RRID:AB_262011
Phospho-p38 MAPK (Thr180/Tyr182) (28B10) antibody	Cell Signaling Technology	Cat#9216; RRID:AB_331296
p38 MAPK Antibody	Cell Signaling Technology	Cat#9212; RRID:AB_330713
Phospho-NF-κB p65 (Ser536) (93H1) antibody	Cell Signaling Technology	Cat#3033; RRID:AB_331284
Anti-GAPDH antibody	Abcam	Cat#ab9485; RRID:AB_307275
Anti-GFAP antibody	Abcam	Cat#ab4674; RRID:AB_304558
TauO specific monoclonal antibody (TOMA2)	Montalbano et al., 2020	N/A
T22 antibody	In-house; Nilson et al., 2017	N/A
AT8, Phospho-Tau (Ser202, Thr205) Antibody	Thermo	Cat#MN1020; RRID:AB_223647
Anti-NeuN Antibody, clone A60 antibody	Chemicon	Cat#MAB377; RRID:AB_2298772
Recombinant Alexa fluor488 anti-NeuN antibody	Abcam	Cat#ab190195, RRID:AB_2716282
Anti-Synapsin I antibody (ab8)	Abcam	Cat#ab8; RRID:AB_2200097
Anti-PSD95 antibody	Abcam	Cat#ab18258; RRID:AB_444362
Goat anti-Rabbit IgG (H+L) Cross-Adsorbed Secondary Antibody, Alexa Fluor 568	Invitrogen	Cat#A-11011; RRID:AB_143157
Goat anti-Rabbit IgG (H+L) Highly Cross-Adsorbed Secondary Antibody, Alexa Fluor 488	Invitrogen	Cat#A-11034; RRID:AB_2576217
Goat anti-Mouse IgG (H+L) Highly Cross-Adsorbed Secondary Antibody, Alexa Fluor 633	Invitrogen	Cat#A-21052; RRID:AB_2535719
Goat Anti-Chicken IgY H&L (Alexa Fluor® 488)	Abcam	Cat#ab150169; RRID:AB_2636803
HRP-conjugated anti-rabbit IgG	GE Healthcare	NA934-1ML; RRID:AB_772206
HRP-conjugated anti-mouse IgG	GE Healthcare	NA93-11ML; RRID:AB_772210
Biological samples		
Human frontal cortex brain tissues from NDC, AD, and FTD patients	The Institute for Brain Aging and Dementia at UC Irvine Puangmalai et al., 2020; Farmer et al., 2020; Montalbano et al., 2020; Nilson et al., 2017	N/A
Escherichia coli BL21(DE3) competent cells	Agilent	Cat# 200131
Chemicals, peptides, and recombinant proteins		
Bovine serum albumin (BSA)	Sigma	Cat# A4161
DMEM	GIBCO	Cat# 11960-044
Triton X-100	Sigma	Cat# T8787
Protease inhibitor cocktail	Sigma	Cat#p8340-1ml

Author Manuscript Author Manuscript Author Manuscript Author Manuscript

REAGENT or RESOURCE	SOURCE	IDENTIFIER
Ethyl pyruvate	Sigma	Cat#8066170100
Glycyrrhizic acid or glycyrrhizin	Sigma	Cat#50531
HBSS	GIBCO	Cat#14175-095
Formaldehyde solution	Sigma	Cat#F8775-500ML
ProLong Gold Antifade reagent	Thermo	Cat#P36935
Fetal Bovine Serum	GIBCO	Cat#1600-044
Goat serum	Cell Signaling Technology	Cat#5425
TauO	Ghag et al., 2018; Puangmalai et al., 2020	N/A
Recombinant HMGB1	Zandarashvili et al., 2013	N/A
DNase I	Biolabs	Cat#M0303S
Antibiotic-Antimycotic (100X)	GIBCO	15240096
Poly-L-lysine solution	Sigma	Cat#P4832
AF568 Protein Labeling kit	Invitrogen	Cat# A10238
PBS	Corning	Cat#46-013-CM
RIPA buffer	Cell Signaling Technology	Cat#9806
Thioflavine S	Sigma	Cat# T1892
Critical commercial assays		
BCA protein assay kit	Pierce	Ca#23225
Cellular Senescence Assay kit	Sigma	Cat#KAA002
Cell cycle analysis: FxCycle™PI/RNase staining	Invitrogen	Cat#F10797
Mouse IL-6 ELISA	Thermo	Cat#88-7064;
Mouse TNF-α ELISA	Thermo	Cat#88-7324;
HMGB1 ELISA	Novus Biologicals	Cat#NBP2-62766
Cation exchange chromatography column	Cytiva	Cat# 29018183
Superdex 200 Increase 10/300 GL	Cytiva	Cat# 28990944
WesternBright ECL HRP substrate	Advanstra	Cat#K-12045-D50
TrueBlack Lipofuscin Autofluorescence Quencher	Biotium	Cat#23007
Deposited data		
Raw immunoblotting images	This paper	https://dx.doi.org/10.17632/765jbfjc5k.1
Experimental models: Organisms/strains		
Mouse: C57LB/6J	Jackson Laboratory	Stock#000664
Mouse: hTau	Jackson Laboratory	Stock#004808
Software and algorithms		
ImageJ	NIH	https://imagej.nih.gov/ij/
BZ-X Analyzer	Keyence	https://www.keyence.com
LSRII Fortessa Analyzer	BD Biosciences	N/A
ANY-maze Behavioral tracking software	ANY-maze	https://www.anymaze.co.uk/index.htm
GraphPad Prism 6	Prism - GraphPad	https://www.graphpad.com